Repetitive Control for Floating Offshore Vertical Axis Wind Turbine

Vimanyu Kumar

Masters Thesis

TU Delft Delft University of Technology

Delft Center for Systems and Control

Repetitive Control for Floating Offshore Vertical Axis Wind Turbine

For the degree of Master of Science in Systems and Control at Delft University of Technology

Vimanyu Kumar

August 28, 2017

Faculty of Mechanical, Maritime and Materials Engineering (3mE) · Delft University of Technology

Copyright © Delft Center for Systems and Control (DCSC)
All rights reserved.

Delft University of Technology
Department of
Delft Center for Systems and Control (DCSC)

The undersigned hereby certify that they have read and recommend to the Faculty of Mechanical, Maritime and Materials Engineering (3mE) for acceptance a thesis entitled

Repetitive Control for
Floating Offshore Vertical Axis Wind Turbine

by

Vimanyu Kumar

in partial fulfillment of the requirements for the degree of
Master of Science in Systems and Control.

Dated: August 28, 2017

Supervisors:

Dr. ir. J.W. van Wingerden

Ir. Feike Savenije

Readers:

Dr. D. Ragni

Ir. MSc. S.P. Mulders

Abstract

The growing importance of renewable energy to meet the demands of growing population has driven much focus for research in the wind energy sector. Currently most of the power production in the wind energy sector is done using the Horizontal Axis Wind Turbine (HAWT) due to its higher efficiency and reliability as compared to Vertical Axis Wind Turbine (VAWT). However, due to limitations of HAWTs such as the complex yaw mechanism, higher positioning of the center of mass and relatively difficult up-scaling, VAWTs are receiving more attention.

Attempt to access high range of power from VAWTs at offshore locations may damage the turbine blades due to increased loads. This thesis is dedicated to reduce the periodic disturbances on the turbine blades of VAWTs without affecting the total power production in a rotation, thereby ensuring the reliability and safe operation of VAWTs. A control technique called Subspace Predictive Repetitive Control (SPRC) is used for the recursive identification to estimate the parameters of wind turbine model and further providing an optimal control law accordingly. Basis functions have been used to reduce the dimensionality of the system, following which the system identification has been performed in the lifted domain.

Using the identified model, two types of control approaches have been applied. In the first approach, the objective function is to track a specific reference that indicates blade load. This reference ensures a reduction in peak loads of the VAWTs by transferring the loads from their upstream to their downstream part, without comprising on the power production in one whole rotation of VAWT. In the second approach, a general control strategy is used in which the controller is given freedom to choose the pitch trajectory so as to reduce the blade loads. The controller is specified with a power reference that ensures the maintenance of total power. This strategy allows the turbine to be operated in different wind conditions, as a higher weighting is assigned to power

production when wind speeds are less than rated wind speeds, and a higher weighting is assigned to the reduction of blade load when wind speeds are more than the rated wind speeds.

These results show a real potential of the data-driven SPRC approach in wind turbines, and highlights new mechanisms to reduce the turbine loads on VAWTs. These mechanisms offer valuable insights into enhancing the functions of VAWTs in a more reliable and damage-free manner.

Table of Contents

List of Figures

List of Tables

Preface

The work presented in this Masters Thesis has been carried out by Vimanyu Kumar, as part of the curriculum for obtaining a Masters degree in Systems & Control at TU Delft. The literature survey is part of my graduation thesis, "Repetitive Control for Floating Offshore Vertical Axis Wind Turbine (VAWT)". It is a joint project at TU Delft and ECN (Energy Research Centre of the Netherlands). I would like to express my gratitude to my supervisors (Ir. Feike Savenije (at ECN) and dr. ir. J.W. van Wingerden (at DCSC)) for giving me a fantastic opportunity to work on this exciting and challenging thesis project. I would also like to thank my parents, brother (Mohit Kumar Jolly) and sister-in-law (Gargi Srivastava Jolly) for their unconditional support, guidance and love which motivated me for the thesis.

Vimanyu Kumar August, 2017

"Of all the forces of nature, I should think the wind contains the largest amount of motive power—that is, power to move things. Take any given space of the earth's surface— for instance, Illinois; and all the power exerted by all the men, and beasts, and running-water, and steam, over and upon it, shall not equal the one hundredth part of what is exerted by the blowing of the wind over and upon the same space. And yet it has not, so far in the world's history, become proportionably valuable as a motive power. It is applied extensively, and advantageously, to sail-vessels in navigation. Add to this a few windmills, and pumps, and you have about all. … As yet, the wind is an untamed, and unharnessed force; and quite possibly one of the greatest discoveries hereafter to be made, will be the taming, and harnessing of it."

— *Abraham Lincoln*

Chapter 1

Introduction

1-1 Motivation

The increasing demand for energy and a limited amount of fossil fuel available on the planet have motivated the scientists to explore renewable sources of energy. Moreover, burning of the fossil fuels is the biggest cause of global warming (1). This demand has generated much drive to move towards sustainable energy (like wind energy) which is renewable, has a lot of potential and produces no greenhouse gases during their operation.

Wind energy is one of the major reserves for sustainable energy and the scientists are working hard to exploit its advantages. According to the Global Wind Energy Council (GWEC) report, the cumulative global wind power capacity has been increased by 12.6%, reaching 486.6 GW in 2016 (2).

According to Siemens (3), the onshore wind turbine accounts for 97% of the global wind power installations due to its various advantages like cheap foundations and easy integration of onshore wind turbines with the electric grid (as compared to the offshore wind turbines). However, onshore wind turbines face many difficulties such as availability of the land for expansion of wind turbines and various obstructions like high buildings which increase wind turbulence. These reasons have led to a shift in the trend to move towards offshore wind locations. To access high range of power (5-10 MW) from these offshore locations, floating structure for offshore wind turbines is used.

Currently, most of the power production is done by the Horizontal Axis Wind Turbine (HAWT)s due to their higher efficiency and increased reliability as compared to

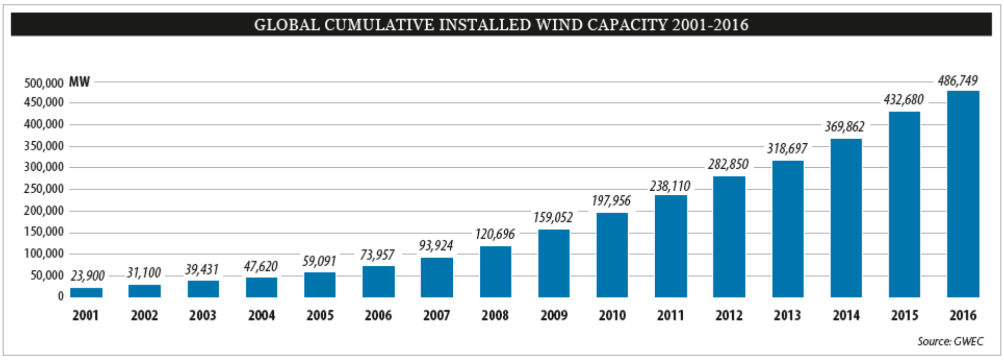

Figure 1-1: Global cumulative wind power capacity according to GWEC report

the Vertical Axis Wind Turbine (VAWT)s. However, there are several advantages of VAWTs over HAWTs which motivate their usage. Some of the advantages are:

- They don't need yaw mechanism.
- The generator, gearbox and other components can be placed on the ground which results in lower Center of Gravity (COG) and thus giving more structural reliability.
- They do not require tall towers, which makes their installation and maintenance easier.
- They don't have to point in the wind for their start up.
- They can face more gusty weather (as compared to HAWT) while maintaining the safety of the blades.
- The upscaling in VAWTs is relatively eaiser.

However, large amounts of energy from VAWT at offshore locations requires large rotor diameters which also means large fatigue loads on the turbine blades. These fatigue loads can destroy the turbine blades (or increase the cost production to manufacture turbines capable of handling these high loads). This possibility can be prevented by pitching the blades in such a way that loads on the turbine blades decrease. But this approach could also reduce the power production of the turbine. So, we need a control algorithm for the blades pitch which not only results decreased fatigue loads but also ensures that power production is not hampered.

1-2 State of the art

A good description of the system is needed to develop a controller. One way to describe the system is to use the model based approach which linearizes the complex aerodynamic equations around the fixed operating point of wind speed (4). However, a linearized model fails to incorporate all the characteristics of the actual non-linear system. Moreover, sometimes, the non-linear model has some unmodelled dynamics at high frequencies which affects the design of the controller. Further, the wind speed is always changing which makes the wind turbine a time varying system. Hence, the modelling of complex systems such as wind turbines is rarely exact (5). Generally, a Linear Parameter Varying (LPV) controller is used to handle these systems [(6), (7)]. But the turbulence and non-linear aerodynamics are quite difficult to predict. It is impossible to design a single LPV controller which works optimally for the wind turbine even with the robust control techniques (8). Due to these reasons, model based approach is not a valid option for describing the linearized model of wind turbine.

Another approach to develop the controller is using the direct data-driven approach [(9), (10)]. In this approach, the system parameters are identified from the persistent excitation of the pitch activity. Further, an optimal controller is derived from the identified parameters. The changing dynamics due to the time varying wind speed can be taken into account by making the system identification adaptive. Further, the controller will adjust itself for the adaptive parameters (11). One of the major advantages of this approach is that there is no longer any requirement of linearizing the aerodynamic equations. This advantage saves a lot of effort and even makes the system parameters more reliable.

The literature survey helped in gaining the useful insights for thesis by indicating the importance of data-driven approach of wind turbines. However, proving the stability of the controlled system for uncertainties poses an open question for data-driven techniques (12). Previous studies showed that the basis functions in the system identification were able to reduce the size of matrices and hence the computational cost (8). Apart from reducing the size of dimensions of the input-output data points, basis functions are also used in rejection of disturbance. It is achieved by expressing the disturbance in the form of the linear combination of basis functions. It helps in selective rejection of the harmonics of the disturbance (13).

Various reports also highlighted the concepts of the lifted domain and the repetitive control for the processes having the periodic properties with the varying initial conditions [(14), (15), (16), (17)]. It has also been shown that the repetitive control was able to reject the periodic disturbances and also track the signals (if needed) (15). The subspace identification allows the derivation of the controller directly from the subspace predictor (18). A combination of subspace identification and predictive control was introduced (known as Subspace Predictive Control (SPC)) by Favoreel *et sl.* (19). Navalkar *et al.* (8) combined the technique of SPC and repetitive control (to develop a technique named as Subspace Predictive Repetitive Control (SPRC)) and implemented it on wind turbines to achieve significant blade load reduction.

1-3 Problem Formulation

Considering the same rotor speed, the wind turbine faces the same blade loads and wind disturbance after every rotation. This arrangement makes the loads and the disturbance in the wind turbine periodic and motivates to use Repetitive Control. So, if the wind turbine system is lifted to the number of samples in the whole rotation, then the periodic wind disturbance would be translated to a constant disturbance (thus simplifying the problem). However, if the number of samples in the rotation is too much, the size of matrices in the lifted domain would increase drastically, thus leading to a large and a complex optimization problem.

The concepts of lifted system and the repetitive control have given promising results for HAWTs (8). Moreover, just like the HAWTs, VAWTs also have the properties of the periodic systems. The shape of blade loads of the VAWTs is also sinusoidal which motivates the use of basis functions to reduce the system dimensionality and further perform the system identification and the controller synthesis (to obtain the optimized pitch trajectory) in the reduced domain. HAWT uses the constraint of summation of the blade pitching at any instant to be zero to ensure same power while reducing the blade loads. However, this condition is not possible in the VAWTs due to cyclic variation of the angle of attack. So, some other constraint on pitching have to be imposed to ensure same power production in VAWTs. In this context, the two specific objectives for this thesis are described below:

- ***Performing data driven learning control on VAWT to ensure reduction of the periodic loading on the blades without compromising the power production per cycle.*** As discussed, data driven approach is a two step process including the system identification and controller synthesis. Exploiting the property of periodic system in wind turbines, repetitive controller in lifted domain will be used. An optimization problem needs to be formulated to represent a trade-off between the blade loads and the power production of the VAWT. This optimization would yield an optimum pitching action (control input) on the blades to achieve the desired objective.

- ***Reducing the complexity and the computational time of the control algorithm by performing the system identification and the controller synthesis in the reduced dimension.*** Performing the data based approach in lifted domain may lead to high dimensionality of the matrices which will increase the computational time drastically. However, wind turbine system being a dynamically varying system needs proper pitching actions at a rapid rate. The sinusoidal basis functions can help to project the high dimensional matrices into the reduced space. The identification and controller design can be performed in this projected space. Finally the controller response can be translated back into the original domain to perform proper pitching actions on the blade.

1-4 Outline

- **Chapter 2** gives a brief introduction about the aerodynamics of the VAWTs and also various streamtube models to analyze the performance of the wind turbines. It will also discuss the basic dynamics of Jeffcott Rotor.
- **Chapter 3** explains the theoretical framework followed in the thesis. All the theoretical concepts will be explained in detail. The two control approaches along with the derivation of LQ Tracker algorithm will be discussed in this chapter.
- **Chapter 4** presents the results when the theoretical framework has been applied to the wind turbines. It will compare the result of the two control approaches followed.
- **Chapter 5** discusses the results obtained in the thesis. It will also answer research questions in the thesis and discusses the possible future work.

Chapter 2

Model Description

The aim of the thesis is to use the control techniques on the model of Vertical Axis Wind Turbine (VAWT) to achieve the optimal pitch trajectory for the blades. However, it is a good practise to test the concepts of these techniques first on a simple system which has some similar properties as a wind turbine i.e. it should have periodic disturbance. The model of Jeffcott Rotor fulfills this criterion and is described in the next section.

This chapter introduces the two different types of systems being worked on i.e. the Jeffcott Rotor and a simplified model of a VAWT. The inputs and outputs to be used for analyzing these systems will be explained in detail.

2-1 Jeffcott Rotor

A simple model for the rotor is a single Degree Of Freedom (DOF) model in which we assume a flexible support with a rigid rotor. The model of the rotor assumes that the geometrical center and center of gravity are coincident. However, in reality, due to operational wear and tear, repairs and manufacturing tolerances, the rotor is no longer perfect and results in an unbalanced force given as:

$$f(t) = m\omega^2 esin(\omega t) \tag{2-1}$$

Here, rotor mass is represented by 'm', rotor speed by 'ω' and 'e' represents the eccentricity of the rotor. Such type of unbalance is often refereed as *inherent unbalance.* An assumption is made that the rotor will perform a simple harmonic motion and it's free response is given by (20) as:

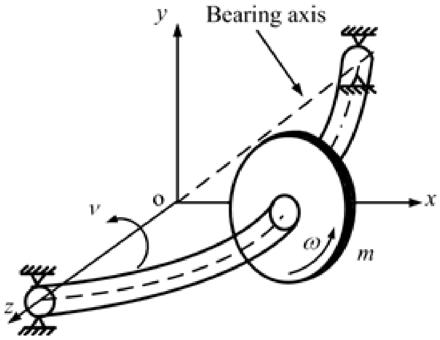

Figure 2-1: Model of Jeffcott Rotor

$$y(t) = Ysin(\omega_n t) \tag{2-2}$$

Here, ω_n represents the natural frequency of the system. Using Newton's second law of motion:

$$m\ddot{y} = -k_{eff}y + m\omega^2 esin(\omega t) \tag{2-3}$$

where '$k_{eff}y$' represents the restoring force with 'k_{eff}' being the effective stiffness of the system. Using 2-2 and 2-3, the natural frequency can be described as:

$$\omega_n = \sqrt{\frac{k_{eff}}{m}} \tag{2-4}$$

The effect of the damping can also be considered in the single DOF Damped Rotor Model (20). However, one of the major limitations of single DOF model is that it fails to express the orbital motion in two transverse directions. Rankine (20) presented the model which uses a two DOF model which expresses the orbital motion of the rotor in the two directions. However, Rankine Model fails to express the realistic rotating unbalance force.

Jeffcott presented a rotor model to get rid of these limitations (Figure 2-1). Jeffcott rotor consists of a mass-less flexible shaft with a rigid disc which is mounted at the mid span (20). The shaft spins with the speed is represented by 'ω' and the whirling frequency (the frequency with which the shaft whirls around the bearing axis) is represented by 'v'. The transverse stiffness ('k') of the shaft is given as:

$$k = \frac{Load}{Deflection} = \frac{P}{PL^3/(48El)} = \frac{48El}{L^3} \tag{2-5}$$

From Figure 2-2, the moment balance around the different axes can be done as:

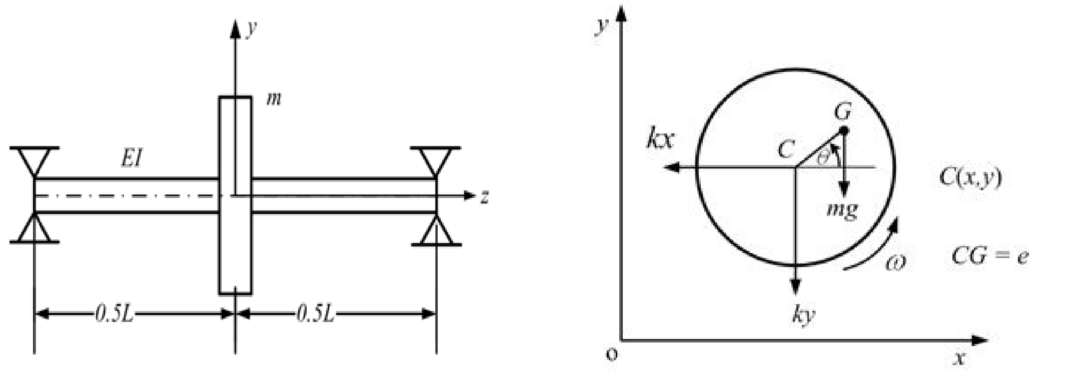

(a) Jeffcott rotor model in y-z plane **(b)** Free body diagram of disc in x-y plane

Figure 2-2: Analysis of Jeffcott Rotor

$$-kx - c\dot{x} = m\frac{\mathrm{d}^2(x + ecos(\theta))}{\mathrm{d}t^2} \tag{2-6}$$

$$-ky - c\dot{y} - mg = m\frac{\mathrm{d}^2(y + esin(\theta))}{\mathrm{d}t^2} \tag{2-7}$$

$$-mgcos(\theta) = I_p\,\ddot{\theta} \tag{2-8}$$

Here $(x + ecos(\theta))$ and $(y + esin(\theta))$ represent the position of the centre of gravity , 'c' is the viscous damping coefficients and I_p represents the polar mass moment of inertia of the disc. Considering a 2 DOF rotor model, the equations of motion can be expressed as:

$$m\ddot{x} + c\dot{x} + kx = m\omega^2 ecos(\omega t) \tag{2-9}$$

$$m\ddot{y} + c\dot{y} + ky = m\omega^2 esin(\omega t) \tag{2-10}$$

Equations 2-9 and 2-10 represent the second order equations of the decoupled motion of Jeffcott rotor in x and y directions. The 2-DOF rotor Jeffcott Rotor model works on a constant rotational speed and has an unbalanced force (represented by the eccentricity). This unbalanced force can be considered as a periodic dynamics (in the Jeffcott model) which has to be rejected. Further, the second model on which the controller techniques have been applied is the simplified model of the VAWT. The next section describes the details of the wind turbine model used for the thesis.

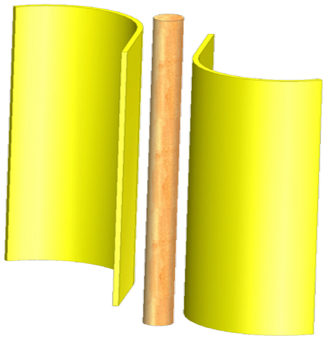

(a) Savonius Turbine

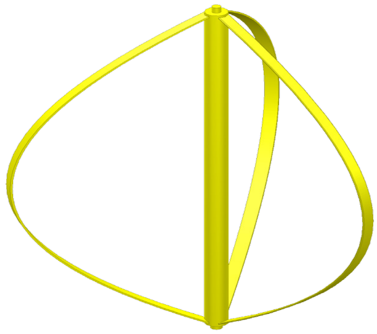

(b) Darrieus Turbine

Figure 2-3: Types of VAWTs

2-2 Simplified model of VAWT

In VAWT, the main rotor shaft is set transverse to the direction of the incoming wind while the other main components are located at the base of the turbine. This setup allows the heavy generator and the gearbox to be located close to the ground, resulting in the lower position of Center of Gravity (COG), giving higher structural stability and easier maintenance (as compared to HAWTs).

Generally, two types of VAWTs are considered: Savonius Turbine and Darrieus Turbine. Savonius Turbines have two (or more) half drums fixed to the shaft in opposite directions (Figure 2-3a, (21)). They are drag-type wind turbines and rotate at low speed. They give high torque, however the maximum efficiency of these turbines is below 25%. On the other hand, Darrieus Turbines (shown in Figure 2-3b, (21)) are lift-force turbines and have higher efficiency than Savonius Turbines. Due to this reason, they are used for high power applications. So, a Darrieus type wind turbine will be considered for the analysis of the thesis.

Various streamtube models are used to evaluate the aerodynamic performance of VAWT. Blade Element Momentum theory (BEM) predicts the power output of VAWT with a high accuracy (for lower tip speed ratios). These streamtube models are used to calculate the thrust force acting on the streamtube by using the conservation equations of mass, momentum and energy. Further, they can be used to solve the flow velocity field in the streamtube.

Each streamtube connects both inlet and outlet and is parallel to the velocity of the flow. Thus, there is no exchange of mass, momentum or energy between the adjacent streamtubes. The flow of the turbine is treated as unidirectional. The mass, momentum and energy conservation equations in the integral form are written in Equations 2-11, 2-12 and 2-13.

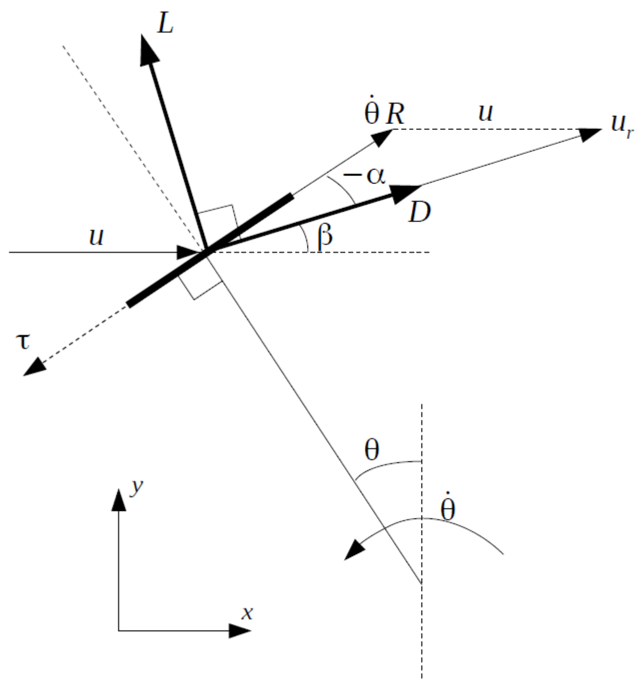

Figure 2-4: Flow velocities and forces acting on VAWT

$$\frac{d}{dt}\int_{\Omega}\rho dV + \oint_{\partial\Omega}\rho\,\mathbf{u}\,.\,\mathbf{n}\,dS = 0, \tag{2-11}$$

$$\frac{d}{dt}\int_{\Omega}\rho\,\mathbf{u}\,dV + \oint_{\partial\Omega}\rho\,\mathbf{u}\,(\mathbf{u}\,.\,\mathbf{n})\,dS = \sum F_{ext}, \tag{2-12}$$

and

$$\frac{d}{dt}\int_{\Omega}\rho\,u^2\,dV + \oint_{\partial\Omega}\frac{1}{2}\rho\,u^2(\mathbf{u}\,.\,\mathbf{n})\,dS = -P \tag{2-13}$$

where Ω represents the domain where the above equations can be applied with **n** being a unit vector normal to $\partial\Omega$ pointing outwards. $\sum F$ is the summation of the forces received by the flow and P is the power output of the part of the turbine within the specified domain.

Figure 2-4 shows the analysis of basic forces acting on a VAWT airfoil. Here, ‘L’ is the lift force, ‘D’ is the drag force, ‘α’ is the angle of attack, ‘β’ is the flight path angle, ‘u_r’ is the relative blade velocity, ‘u’ is the wind speed at the blade, ‘R’ is the radius of blade and ‘τ’ is the unit vector in the tangential direction of blade. The lift force is perpendicular to the relative blade velocity whereas the and the drag force is in the direction of the relative velocity. The relative blade velocity (u_r) can be written as:

$$\frac{u_r}{U_\infty} = \sqrt{\left(\frac{u}{U_\infty}\right)^2 + (TSR)^2 + 2\frac{u}{U_\infty}\,TSR\,cos(\theta)} \tag{2-14}$$

where TSR (Tip Speed Ratio) is the ratio of the tip velocity of the blade to the actual wind speed. The flight path angle can be given as:

$$\beta = arctan\left(\frac{TSR\,sin(\theta)}{u/U_\infty + TSR\,cos(\theta)}\right) \tag{2-15}$$

The angle of attack (α) can be given as:

$$\alpha = modulus\left(\frac{\pi + \beta - \theta}{2\pi}\right) \tag{2-16}$$

Now, the lift and the drag coefficients (respectively given by C_L and C_D) can be calculated from the experimental data:

$$L = \frac{1}{2}\rho c u_r^2 C_L \tag{2-17}$$

$$D = \frac{1}{2}\rho c u_r^2 C_D \tag{2-18}$$

The total force perceived by the blades can be wrtiten as:

$$F = [Dcos(\beta) - Lsin(\beta)]i + [Dsin(\beta) + Lcos(\beta)]j \tag{2-19}$$

This force can be used to calculate the torque contribution by each blade:

$$T = RF \cdot t = R(Ll + Dd) \cdot \tau \tag{2-20}$$

where $l = -sin(\beta)i + cos(\beta)j, d = cos(\beta)i + sin(\beta)$ and $\tau = -cos(\theta)i - sin(\theta)$.

2-2-1 Double Multiple Streamtube Model (DMST)

DMST is considered as the most precise streamtube model because it allows to compute the energy losses of the flow separately for front and rear part of the VAWT. It considers the flow to be travelling through the two consecutive actuator disks which are responsible for extracting the energy. The turbine is divided into the various multiple streamtubes parallel to the flow (22).

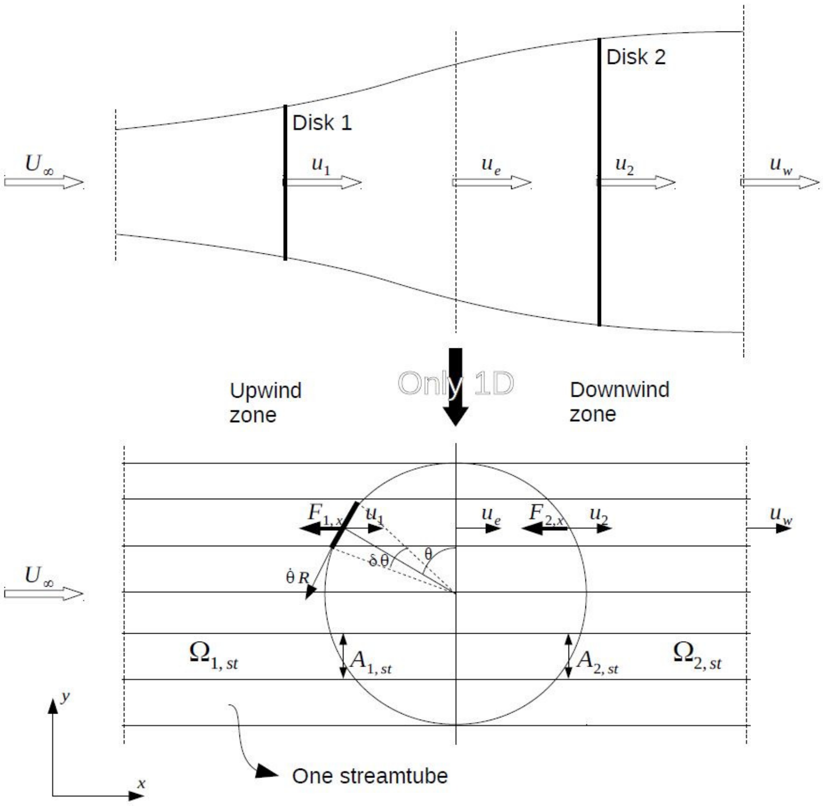

Figure 2-5: Schematic representation of DMST scheme

A schematic of DMST is shown in Figure 2-5. It can be seen that the flow has various states. The state '∞' is not disturbed by the turbine and acts as the input for Disk 1. State '1' interacts with the upwind actuator disk and is called front half cycle of VAWT. State 'e' describes the equilibrium state as DMST assumes the flow in this state to be far away from states **1** and **2**. State '2' represents the interaction with the downwind actuator disk and state 'w' is the wake state which acts as the output for Disk 2 (22).

The conservation equations for mass, momentum and energy are applied independently for front and rear streamtubes. Considering $A_{i,st}$ being the area for each streamtube, the mass balance is given by Equation 2-21.

$$\dot{m} = \rho u_1 A_{1,st} = \rho u_2 A_{2,st} \tag{2-21}$$

Using Equation 2-12, the momentum balance for front and rear streamtubes is given by Equation 2-22 and 2-23.

$$\dot{m}(u_e - U_\infty) = -F_{1,x}, \tag{2-22}$$

$$\dot{m}(u_w - u_e) = -F_{2,x}, \tag{2-23}$$

Similarly from Equation 2-13, the energy balance for both the streamtubes is given by Equation 2-24 and 2-25.

$$\frac{1}{2}\dot{m}(u_e^2 - U_\infty^2) = -F_{1,x}u_1 \tag{2-24}$$

$$\frac{1}{2}\dot{m}(u_w^2 - U_e^2) = -F_{2,x}u_2 \tag{2-25}$$

Using the above equations, the velocity in the states of equilibrium and wake can be given as:

$$u_e = U_\infty(2\lambda_1 - 1), \tag{2-26}$$

$$u_w = u_e(2\lambda_2 - 1) \tag{2-27}$$

where $\lambda_1 = u_1/U_\infty$ and $\lambda_2 = u_2/u_e$.

The thrust acting on the turbine at a given azimuth angle can be given by the following equation:

$$F_{i,x}(\theta) = \frac{1}{2}\rho c u_{i,r}^2(C_D cos\beta - C_L sin\beta), \quad \forall i = 1,2 \tag{2-28}$$

2-2-2 Dynamic Stall

Dynamic stall has a relevant role in the dynamics of VAWT. It refers to the phenomenon when the lift force starts to decrease with very high angles of attack. It is an important concept and needs to be included in VAWT model. Generally, DMST has a series of semi-emperical procedures to calculate the lift and drag coefficients (23). Gormont (24) proposed to consider dynamic stall in helicopter blades for VAWT. However, the helicopter blades operate at higher angles of attack and is not optimal for VAWT. Further, Berg (25) proposed some modification for the calculation of lift and drag coefficients. Strickland *et al.* (26) modified the delay of Gormont model to account for higher thickness over chord ratio of VAWT blades. The Gormont model has been used in the thesis for the analysis of VAWT model.

2-2-3 Wake Interaction

Wake interaction represents the effect of the turbulent wakes generated by the front half of the turbine and received on the rear half. The concept of wake interaction is neglected in the streamtube models. Kozak *et al.* (27) realized that the number of wakes in the rear half is proportional to the Tip Speed Ratio (TSR) and number of blades. Kozak and Vallverdu observed that each blade is hitting each wake twice and considered that the width of a wake equals to that of blade thickness. This allows the distance value to be calculated as:

$$d_w = 2\ t\ N_w \tag{2-29}$$

Here d_w is the summation of all parts of turbine blades path which crosses the wake. To represent it more clearly, a ratio is defined as:

$$r_w = \frac{d_w}{\pi R} \tag{2-30}$$

Kozak *et al.* (27) assumed that the flow in the wake travels with same speed and direction as was generated by the blade. This would mean that the relative velocity and instantaneous angle of attack will be diminished. However in reality, the direction of wake and blade is not parallel. To account for this, the angle of attack of the rear part was multiplied with a term $(1 - r_w)$ by Kozak and Vallverdu *et al.* (27) and is used in the VAWT model for thesis.

2-2-4 Model Description

The above mentioned aerodynamics of VAWT has been implemented in the given simplified model at Energy research Centre of the Netherlands (ECN). As discussed, the aim of the thesis is to find an optimal pitch trajectory to reduce the loads on the turbine while extracting constant power from the turbine. However, dealing with the non-linear dynamics of wind turbine while designing the controller is a quite difficult task. One of the solutions is to linearize the dynamics of VAWT around some operating points and consider the linearized system for control. However, as the wind speeds are changing, we would have various linearized models of wind turbine and then we may use more than one Linear Parameter Varying (LPV) controller. The linearized model does not completely represent all the dynamics of the wind turbine. Moreover, even the non-linear model cannot model all the uncertainties in the wind turbine. Further, the behaviour of the system at high frequencies changes the system dynamics. Due to these difference between modelled system and real world, the model based approach cannot give the optimum control law for the wind turbines.

So, a technique called as data-driven approach (which involves persistent excitation of the input i.e. pitch angle for the wind turbine, to determine the model dynamics) treats the system as black-box and thus saves all the effort of linearizing the aerodynamic equations. It also relieves us from the dependency of the accuracy of the available model. However, a proper excitation is required to perform system identification in the data-driven approach. Moreover, a re-identification of parameters is needed with changing wind speeds. To overcome these limitations, a simultaneous identification and control strategy is followed to re-identify the system parameters and provide an optimal control law accordingly. A forgetting factor is implemented (in the thesis) in the identification process to ensure the identified parameters remain adaptive with changing dynamics. Considering these arguments, the focus of the thesis is to use the data-driven approach for VAWTs.

Figure 2-6 shows the structure of the data-driven scheme to be followed. The pitch angles (control inputs) and the wind (disturbance input) act as an input to the wind turbine model, with the blade loads and power production as the outputs from VAWT. The closed loop controller gives the control law for the optimum pitch trajectories to meet the objectives.

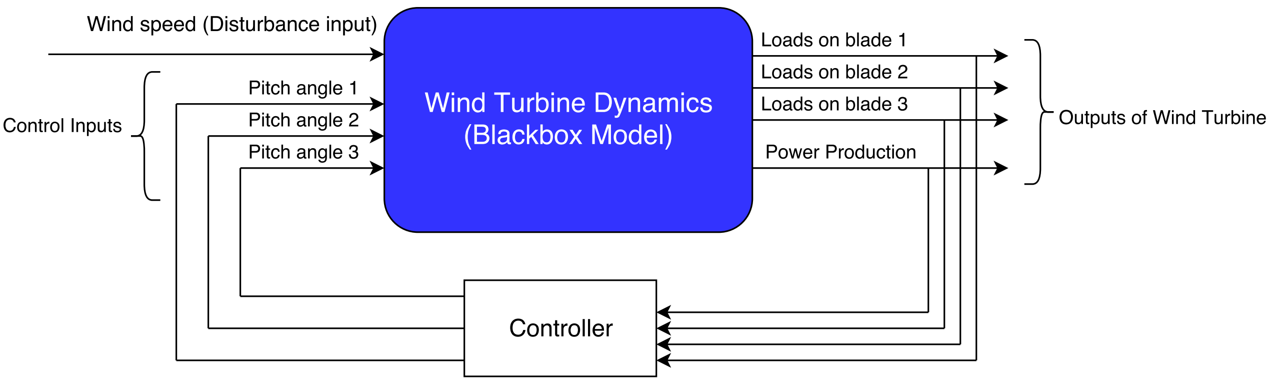

Figure 2-6: Structure of data-driven approach in VAWT

Chapter 3

Theoretical Framework

This chapter starts with introducing the general control strategy followed in the control of wind turbines. Further, it describes the identification procedure in reduced domain. It also describes the concept of lifted domain and how repetitive control is able to solve the problem of periodic disturbance. The concept of basis functions in reducing the dimensionality will be discussed. Further, two control approaches will be discussed that can match the objectives.

3-1 Control of Wind Turbines

According to the different wind speed the turbine encounters, the generator torque must be controlled in such a way to achieve the desired trajectory of the power and the rotor speed. Figure 3-1 below shows the desired trajectory (28). At very low wind speeds, the torque exerted by the wind on the turbine blades is insufficient to make them rotate. However, as the wind speed increases, turbine starts to rotate and generate electric power. The wind speed at which the turbine starts to rotate is called **cut-in speed**. As the wind speed rises above cut-in speed, the power generated by the turbine rises rapidly as shown (region I in Figure 3-1). The rated power from turbine is obtained at the wind speed known as **rated speed**. For the wind speeds between cut-in and rated, the wind turbine operates at the optimal power coefficient (C_p) and the rotor speed varies directly with the wind speed. **Cut-out speed** corresponds to the wind speed at which rotor is brought to the standstill. For the wind speeds lying in region III (Figure 3-1), the wind turbine is operated at rated power and rated wind speed. This control is applicable for both the types of turbines (HAWT, VAWT).

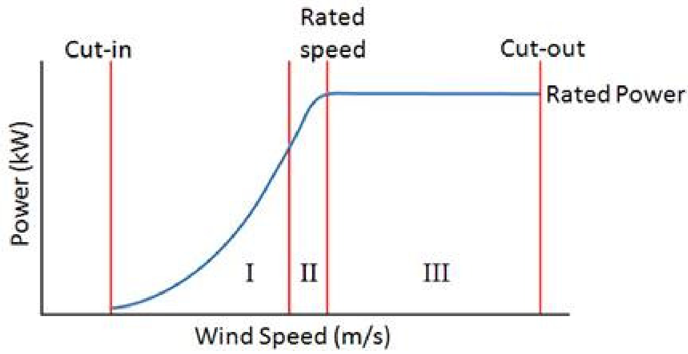

Figure 3-1: Various regions of operations of wind turbine

3-2 Subspace Predictive Repetitive Control (SPRC)

The data driven control approach offers an alternative to the robust model-based controller. It generally involves two steps: a) system identification from the input-output data, and b) synthesis of an optimal control law. This approach requires the persistent excitation to excite the relevant modes of the system. As no parametric model is required to design the optimal control law, this approach is termed as a 'model free approach'.

The technique of SPRC (8) combines the system identification with the implementation of the repetitive controller. SPRC should be able to reject the periodic disturbances in the Vertical Axis Wind Turbine (VAWT) without affecting the power production. The dynamics of the wind turbine system (as a Linear Time Invariant (LTI) system) can be given as :

$$x_{k+1} = \bar{A}x_k + \bar{B}u_k + \bar{E}d_k + Ke_k \tag{3-1}$$

$$y_k = Cx_k + Du_k + Fd_k + e_k \tag{3-2}$$

where x_k is the state vector ($x_k \in \mathbb{R}^n$ where n is the number of states), u_k is the input vector representing the pitch angles of the blades ($u_k \in \mathbb{R}^{nu}$), d_k is the periodic disturbance due to the loading on the blades of turbine ($d_k \in \mathbb{R}^{nd}$) and e_k represents the process noise of the system (i.e. wind disturbance). It can be easily recasted in predictor form as:

$$x_{k+1} = Ax_k + Bu_k + Ed_k + Ky_k \tag{3-3}$$

$$y_k = Cx_k + Du_k + Fd_k + e_k \tag{3-4}$$

where, $\quad A = \bar{A} - KC, \quad B = \bar{B} - KD, \quad E = \bar{E} - KF$

Once the prediction form is done, we need to perform the identification that will be done in the lifted domain (it means according to the time period of the rotor). The next section helps in understanding how to transfer the given problem into the lifted domain.

3-3 Lifted Domain

We require to lift the system matrices to perform identification in the lifted domain. Lifting the above system (Equations 3-3 and 3-4) results the LTI system in form (29):

$$x_{k+N} = A^N x_k + K_u U_k + K_d D_k + K_y Y_k \tag{3-5}$$

$$Y_k = \Gamma x_k + HU_k + \bar{J} D_k + E_k \tag{3-6}$$

The system has been translated into the lifted domain with the window size equal to N where N denotes the number of samples in a rotational period (T_p). Now, the time index 'k' will be replaced by by the iteration index 'j', in such way that $(k, k+N, k+2N, ...) \rightarrow (j, j+1, j+2...)$ (8):

$$x_{j+1} = A^N x_j + K_u U_j + K_d D_j + K_y Y_j \tag{3-7}$$

$$Y_j = \Gamma x_j + HU_j + \bar{J} D_j + E_j \tag{3-8}$$

Here, K_u represents the extended controllability matrix and is represented by :

$$K_u = [A^{N-1}B \quad A^{N-2}B \quad ... \quad B] \tag{3-9}$$

The matrices K_d and K_y also have the similar structure:

$$K_d = [A^{N-1}F \quad A^{N-2}F \quad ... \quad F] \quad \text{and} \quad K_y = [A^{N-1}K \quad A^{N-2}K \quad ... \quad K] \tag{3-10}$$

The Topelitz (H and J) and the extended observability (Γ) matrix are given by :

$$\Gamma = \begin{pmatrix} C \\ CA \\ . \\ . \\ . \\ . \\ CA^{N-1} \end{pmatrix} \tag{3-11}$$

$$H = \begin{bmatrix} D & 0 & . & . & . & . & 0 \\ CB & D & . & . & . & . & 0 \\ . & . & . & & & & . \\ . & . & & . & & & . \\ . & . & & & . & & . \\ . & . & & & & . & . \\ CA^{N-2}B & CA^{N-3}B & . & . & . & . & D \end{bmatrix} \quad , \quad J = \begin{bmatrix} 0 & 0 & . & . & . & . & 0 \\ CF & 0 & . & . & . & . & 0 \\ . & . & . & & & & . \\ . & . & & . & & & . \\ . & . & & & . & & . \\ . & . & & & & . & . \\ CA^{N-2}F & CA^{N-3}F & . & . & . & . & 0 \end{bmatrix} \tag{3-12}$$

The stacked output vector (Y_k) is given in Equation 3-13. The input vector (U_k), disturbance vector (D_k) and the error vector (E_k) are also defined in the same way. It should be noted that the disturbance vector (D_k) is constant.

$$Y_k = \begin{pmatrix} y_k \\ y_{k+1} \\ . \\ . \\ y_{k+N-1} \end{pmatrix} \tag{3-13}$$

For stable wind dynamics, we would have a stable system matrix (A). For a sufficiently large N, we can assume $A^N \approx 0$. This reduces the equation 3-7 to the following form:

$$x_{j+1} = \begin{bmatrix} K_u & K_y & K_d D_j \end{bmatrix} \begin{bmatrix} U_j \\ Y_j \\ 1 \end{bmatrix} \tag{3-14}$$

Substituting the above equation in the equation 3-8, we have:

$$Y_j = \begin{bmatrix} \Gamma K_u & \Gamma K_y & H & (\Gamma K_d + J) D_j \end{bmatrix} \begin{bmatrix} U_j \\ Y_{j-1} \\ U_j \\ 1 \end{bmatrix} + E_j \tag{3-15}$$

It should be noted that E_j is uncorrelated with the output and input values of the previous iteration. In the controller, the lifted control input for the next iteration will be determined at the end of the current iteration. This implies that in the lifted domain, the vector E_j will be an uncorrelated zero-mean white noise (8). It can be seen that for a high value of N (number of samples in a rotation), the problem of identification will grow very large in dimension.

3-4 Basis Functions

The approach of the basis functions can help to map the high input-output data into the lower dimensionality. One of the limitations of the basis function approach is that the dynamics and control of the system can be done only in the limited dimension space. Considering ϕ_u and ϕ_y as the input and output projection matrices, the reduced input and output matrices are given as:

$$U_r = \phi_u U_j, \qquad Y_r = \phi_y Y_j \tag{3-16}$$

An obvious choice of ϕ_u and ϕ_y as the identity matrix can recover the whole original space. The input basis vectors (corresponding to the pitch angles) are used to shape the control input while the output basis vectors (corresponding blade loads or the total power production in a cycle) describe the predicted output of the controller in the limited space which result from the limited-space control of pitch angles. The basis vectors for projecting the input-output data into the limited-space are given by:

$$\phi_u = \phi_y = [\phi_1^T, \quad \phi_2^T, \quad \cdots, \quad \phi_b^T] \tag{3-17}$$

The number of basis vectors are given by b, and generally, $b << N$, so that the size of reduced dimension is much smaller than the lifted system. As the input can have effect on sinusoids in the output of the same frequency, the same basis functions are used to project the stacked input-output data. The original dimensionality of the control input can be recovered by performing the Moore-Penrose pseudo inverse of the projected matrix (30) :

$$U_{k,N} = \phi_u^{\dagger} U_r \tag{3-18}$$

3-5 Choice of basis functions

As we are dealing with periodic systems, we need to choose basis functions which have a periodic nature. The obvious choice that displays a similar nature would be sinosoids of integral multiple of 1P (1P is the frequency at which the rotor rotates). Navalkar *et al.* (8) took the sinusoids of frequencies 1P and 2P and the basis functions were respectively displaced by 120°for the three blades. But this method would just increase the size of the computations as now we have to deal with different basis functions for different blades. So, to reduce the burden on the system, the same basis functions for the three blades should be taken. The structure of the basis functions would be in the following form:

$$\phi_u = \phi_y = \begin{bmatrix} sin(\frac{2*\pi*1*1}{N}) & sin(\frac{2*\pi*1*2}{N}) & \cdot\ \cdot\ \cdot & sin(\frac{2*\pi*1*N}{N}) \\ cos(\frac{2*\pi*1*1}{N}) & cos(\frac{2*\pi*1*2}{N}) & \cdot\ \cdot\ \cdot & cos(\frac{2*\pi*1*N}{N}) \\ sin(\frac{2*\pi*2*1}{N}) & sin(\frac{2*\pi*2*2}{N}) & \cdot\ \cdot\ \cdot & sin(\frac{2*\pi*2*N}{N}) \\ cos(\frac{2*\pi*2*1}{N}) & cos(\frac{2*\pi*2*2}{N}) & \cdot\ \cdot\ \cdot & cos(\frac{2*\pi*2*N}{N}) \\ \cdot & \cdot & \cdot\ \cdot\ \cdot & \cdot \\ \cdot & \cdot & \cdot\ \cdot\ \cdot & \cdot \\ \cdot & \cdot & \cdot\ \cdot\ \cdot & \cdot \\ sin(\frac{2*\pi*np*1}{N}) & sin(\frac{2*\pi*np*2}{N}) & \cdot\ \cdot\ \cdot & sin(\frac{2*\pi*np*N}{N}) \\ cos(\frac{2*\pi*np*1}{N}) & cos(\frac{2*\pi*np*2}{N}) & \cdot\ \cdot\ \cdot & cos(\frac{2*\pi*np*N}{N}) \end{bmatrix} \tag{3-19}$$

where np represents the number of basis functions. The proper weightage on sine and cosine terms of the basis functions ensure that full space corresponding to that integral multiple of 1P can be covered. Higher integral multiples of 1P are used to analyze the higher harmonics in the load signal (8).

Now projecting the equation 3-15 into the projected subspace we have :

$$Y_{r,j} = \begin{bmatrix} \phi_y \Gamma K_u \phi_u^\dagger & \phi_y \Gamma K_y \phi_y^\dagger & \phi_y H \phi_u^\dagger & \phi_y(\Gamma K_d + J) D_j \end{bmatrix} \begin{bmatrix} U_{r,j-1} \\ Y_{r,j-1} \\ U_{r,j} \\ 1 \end{bmatrix} + \phi_y E_j \tag{3-20}$$

3-6 System Identification

The aim of the iteration domain system identification in reduced domain is to predict the projected output based on the past projected input-output data. In order to formulate a regression problem, equation 3-20 is used to define Markov parameters Ξ_r as:

$$\Xi_r = \begin{bmatrix} \phi_y \Gamma K_u \phi_u^\dagger & \phi_y \Gamma K_y \phi_y^\dagger & \phi_y H \phi_u^\dagger & \phi_y(\Gamma K_d + J) D_j \end{bmatrix} \tag{3-21}$$

If the input-output data is available at the current and past iterations (for j and j-1), it is possible to estimate the Markov parameters (Ξ_r) by performing the system identification online in a recursive manner. The identification problem can be put forward in the way as shown:

$$Y_{r,j} = \Xi_r \begin{bmatrix} U_{r,j-1} \\ Y_{r,j-1} \\ U_{r,j} \\ 1 \end{bmatrix} + \phi_y E_j \tag{3-22}$$

Now, a Recursive Least Squares (RLS) approach can be taken to recursively estimate Ξ_r. However, it should be noted that the wind turbine is a dynamically varying system. So, to update the parameters for slow varying wind speeds, a forgetting factor should also be used in the RLS approach to make the identified parameters more adaptive. Thus, estimation of Ξ_r can be formulated as (8):

$$\hat{\Xi}_{r,j} = arg \min_{\Xi_r} \sum_{q=0}^{j-1} \left\| Y_{r,j} - \Xi_r \begin{bmatrix} U_{r,j-1} \\ Y_{r,j-1} \\ U_{r,j} \\ 1 \end{bmatrix} \right\|_2^2 \tag{3-23}$$

It should be kept in mind that the noise E_j is uncorrelated with the input-output data of the current iteration (j). Multiplying, E_j with the projection matrix ϕ_y still renders the noise in projected space uncorrelated with the input-output in projected space. This makes E_j as a white noise sequence in the lifted domain. This makes sure that RLS approach with the forgetting factor (Algorithm 1) in equation 3-23 will give unbiased estimates of Ξ_r (11). However, it should made be sure that the condition of persistent excitation holds. Once an estimate of the projected Markov parameters ($\hat{\Xi}_{r,j}$) is obtained, a proper partitioning can be done to obtain:

$$\hat{\Xi}_{r,j} = \begin{bmatrix} \widehat{\phi_y \Gamma K_u \phi_u^\dagger} & \widehat{\phi_y \Gamma K_y \phi_y^\dagger} & \widehat{\phi_y H \phi_u^\dagger} & \phi_y(\Gamma \widehat{K_d + J}) D_j \end{bmatrix}_j \tag{3-24}$$

Algorithm 1 *Recursive Least Squares with a Forgetting Factor*

1: $P \leftarrow Identity \quad Matrix$
2: $i \leftarrow 1$
3: **while** $i \leq Nr$ **do** ▷ Nr is the number of rotational samples
4: $\quad x_j \leftarrow [U_{r,j-1} \quad Y_{r,j-1} \quad U_{r,j}]$
5: $\quad P_j \leftarrow \frac{1}{\lambda}(P_{j-1} - P_{j-1}x_j x_j^T P_{j-1}(\lambda I + x_j^T P_{j-1} x_j)^{-1})$
6: $\quad \hat{\Gamma}_j \leftarrow \hat{\Gamma}_{j-1} - P_j x_j (Y_{r,j} - x_j^T \hat{\Gamma}_{j-1})$
7: $\quad i \leftarrow i + 1$
8: **return** i

3-7 Repetitive Control

It has been shown that the peak loads in the wind turbines is a periodic process. So, in other words, a controller is required which is able to reject the disturbance in the system periodically. This leaves us the choice of two types of learning controllers: Iterative Learning Control (ILC) and Repetitive Control (RC). However, in case of wind turbines, the initial condition of the periodic process is always changing due to the nature of wind. This motivates the use of a Repetitive Controller.

Van de Wijdeven and Bosgra (31) introduced the general form of RC with basis functions:

$$U_{r,j+1} = \alpha U_{r,j} + \beta \begin{bmatrix} x_{init,j-1} \\ \epsilon_{j-1} \end{bmatrix} \tag{3-25}$$

Here $x_{init,j-1}$ represents the initial condition of the previous iteration, ϵ is the error in disturbance rejection, β is the learning gain matrix and α is the Q-filter for robustness issues. Currently, the Q-filter is not used for this thesis, i.e. $\alpha = 1$. This assumption helps to formulate the problem in difference form which eliminates the effect of constant disturbance (explained later). The output predictor in equation 3-15 can be given as:

$$Y_{r,j} = \begin{bmatrix} (\widehat{\phi_y \Gamma K_u \phi_u^\dagger})_j & (\widehat{\phi_y \Gamma K_y \phi_y^\dagger})_j & (\phi_y (\widehat{\Gamma K_d + J}) D)_j \end{bmatrix} \begin{bmatrix} U_{r,j-1} \\ Y_{r,j-1} \\ 1 \end{bmatrix} + (\widehat{\phi_y H \phi_u^\dagger})_j U_{r,j} \tag{3-26}$$

It can be seen in the Equation 3-26 that the term of the process noise E_j is omitted. Further, an operator δ can be used to eliminate the effect of the constant disturbance (lifted domain), where δ can be defined as:

$$\delta Y_{r_j} = Y_{r,j} - Y_{r,j-1}, \quad \delta U_{r,j} = U_{r,j} - U_{r,j-1}, \quad \delta(1) = 0 \tag{3-27}$$

Using δ in equation 3-26, we have:

$$\delta Y_{r_j} = \begin{bmatrix} (\widehat{\phi_y \Gamma K_u \phi_u^\dagger})_j & (\widehat{\phi_y \Gamma K_y \phi_y^\dagger})_j \end{bmatrix} \begin{bmatrix} \delta U_{r,j-1} \\ \delta Y_{r,j-1} \end{bmatrix} + (\widehat{\phi_y H \phi_u^\dagger})_j \delta U_{r,j} \tag{3-28}$$

These equations can be written in the standard form of a discrete system which can be used to design the stabilizing controller. However, the controller should be designed with the true parameters. So, in the following equations, the hat notation will not be used:

$$\underbrace{\begin{bmatrix} Y_{r,j} \\ \delta U_{r,j} \\ \delta Y_{red,j} \end{bmatrix}}_{\mathbf{x_{j+1}}} = \underbrace{\begin{bmatrix} I_b & (\phi_y(\Gamma K_u)\phi_u^\dagger)_j & (\phi_y(\Gamma K_y)\phi_y^\dagger)_j \\ 0_b & 0_b & 0_b \\ 0_b & (\phi_y(\Gamma K_u)\phi_u^\dagger)_j & (\phi_y(\Gamma K_y)\phi_y^\dagger)_j \end{bmatrix}}_{\mathbf{A_j}} \underbrace{\begin{bmatrix} Y_{r,j-1} \\ \delta U_{r,j-1} \\ \delta Y_{r,j-1} \end{bmatrix}}_{\mathbf{x_j}} + \underbrace{\begin{bmatrix} (\phi_y H \phi_u^\dagger)_j \\ I_b \\ (\phi_y H \phi_u^\dagger)_j \end{bmatrix}}_{\mathbf{B_j}} \underbrace{\begin{bmatrix} \delta U_{r,j} \end{bmatrix}}_{\mathbf{u_j}} \tag{3-29}$$

$$\underbrace{\begin{bmatrix} Y_{r,j} \end{bmatrix}}_{\mathbf{y_j}} = \underbrace{\begin{bmatrix} I_b & (\phi_y(\Gamma K_u)\phi_u^\dagger)_j & (\phi_y(\Gamma K_y)\phi_y^\dagger)_j \end{bmatrix}}_{\mathbf{C_j}} \underbrace{\begin{bmatrix} Y_{r,j-1} \\ \delta U_{r,j-1} \\ \delta Y_{r,j-1} \end{bmatrix}}_{\mathbf{x_j}} + \underbrace{\begin{bmatrix} (\phi_y H \phi_u^\dagger)_j \end{bmatrix}}_{\mathbf{D_j}} \underbrace{\begin{bmatrix} \delta U_{r,j} \end{bmatrix}}_{\mathbf{u_j}} \tag{3-30}$$

Once the equations have been represented in the standard form, the controller needs to be designed. Two possible control strategies are discussed. First one involves defining the reference for the blade loads with the help of basis functions in such a way that the peak load of the blade is reduced (in upstream) and that the reduction is compensated by the increase of load at other location (in downstream) to maintain constant power production. A different set of references can be set and then we can use a LQ tracker algorithm (derived in section 3-8) to track the reference.

Another approach involves giving a proper reference to the power (which equals the power before applying control) and a zero reference to the loads. Further, a high weighting can be used for the reference of power to keep the power same while the peak loads are reduced. Also, instead of giving a proper power trajectory, the reference of total power in a period is given. In this way, the controller has more freedom to optimize the pitch trajectory. A proper choice of having proper basis function should be made to convert total power in a rotation into the reduced domain and then perform the system identification for the total power production. An obvious choice of such basis function is a constant equal to unity. It can be easily verified in the following equation:

$$P_{r,j} = \begin{bmatrix} 1 & 1 & \cdots 1_N \end{bmatrix} \begin{bmatrix} P_{j1} \\ P_{j2} \\ \vdots \\ P_{jN} \end{bmatrix} \tag{3-31}$$

Here P_{ji} (where i=1,2.... N represent the indices of P) represents the power of ith sample for jth rotation of wind turbine with N being the number of samples in a rotation. It can be easily seen that the $P_{r,j}$ represents the summation of all power samples of jth

rotation and its size in reduced domain is 1. This allows us to take the basis function for the total power (in a whole period) as (ϕ) :

$$\phi = \begin{bmatrix} 1 & 1 & \cdots & 1_N \end{bmatrix} \tag{3-32}$$

However, unlike individual blade loads, the identification of the total power production (in a period) would require the pitch angles of all the three blades. The output predictor for the summation of the power in the whole rotation can be given as (compare it to equation 3-23):

$$\hat{\Xi}_{p,r,j} = arg \min_{\Xi_{p,r,j}} \sum_{i=0}^{j-1} \left\| P_{red} - \Xi_{p,r,j} \begin{bmatrix} U1_{r,j-1} \\ U2_{r,j-1} \\ U3_{r,j-1} \\ P_{r,j-1} \\ U1_{r,j} \\ U2_{r,j} \\ U3_{r,j} \\ 1 \end{bmatrix} \right\|_2^2 \tag{3-33}$$

where U1, U2 and U3 represent the projected pitch angles corresponding to the three blades. Once, an estimate of the projected Markov parameters ($\hat{\Xi}_{p,r,j}$) is obtained, a proper partitioning can be done to obtain:

$$\hat{\Xi}_{p,r,j} = \begin{bmatrix} \phi\widehat{\Gamma_p K_{up}}\phi^\dagger & \phi\widehat{\Gamma_p K_{yp}}\phi^\dagger & \widehat{\phi H_p \phi^\dagger} & \phi(\Gamma_p \widehat{K_{dp} + J_p})D_{jp} \end{bmatrix}_j \tag{3-34}$$

After identifying the power production term of the wind turbine, we can give the reference as the power production per cycle and a zero as the reference to the blade loads.

Once the identification of the projected blade loads and the projected total power (in a rotation) has been done, the control formulation needs to be done. Unlike in equation 3-30, the output in this approach would be the projected loads of all the blades including the projected power in a rotation.

$$
\underbrace{\left[\begin{array}{c} Y1_{r,j} \\ \delta U1_{r,j} \\ \delta Y1_{r,j} \\ \hline Y2_{r,j} \\ \delta U2_{r,j} \\ \delta Y2_{r,j} \\ \hline Y3_{r,j} \\ \delta U3_{r,j} \\ \delta Y3_{r,j} \\ \hline P_{r,j} \\ \delta P_{r,j} \end{array}\right]}_{\mathbf{xp_{j+1}}} = \underbrace{\left[\begin{array}{ccc|ccc|ccc|cc}
I & \phi_y\widehat{\Gamma_1\bar{K}_{u1}}\phi_u^\dagger & \phi_y\widehat{\Gamma_1\bar{K}_{y1}}\phi_y^\dagger & 0 & 0 & 0 & 0 & 0 & 0 & 0 & 0 \\
0 & 0 & 0 & 0 & 0 & 0 & 0 & 0 & 0 & 0 & 0 \\
0 & \phi_y\widehat{\Gamma_1\bar{K}_{u1}}\phi_u^\dagger & \phi_y\widehat{\Gamma_1\bar{K}_{y1}}\phi_y^\dagger & 0 & 0 & 0 & 0 & 0 & 0 & 0 & 0 \\ \hline
0 & 0 & 0 & I & \phi_y\widehat{\Gamma_2\bar{K}_{u2}}\phi_u^\dagger & \phi_y\widehat{\Gamma_2\bar{K}_{y2}}\phi_y^\dagger & 0 & 0 & 0 & 0 & 0 \\
0 & 0 & 0 & 0 & 0 & 0 & 0 & 0 & 0 & 0 & 0 \\
0 & 0 & 0 & 0 & \phi_y\widehat{\Gamma_2\bar{K}_{u2}}\phi_u^\dagger & \phi_y\widehat{\Gamma_2\bar{K}_{y2}}\phi_y^\dagger & 0 & 0 & 0 & 0 & 0 \\ \hline
0 & 0 & 0 & 0 & 0 & 0 & I & \phi_y\widehat{\Gamma_3\bar{K}_{u3}}\phi_u^\dagger & \phi_y\widehat{\Gamma_3\bar{K}_{y3}}\phi_y^\dagger & 0 & 0 \\
0 & 0 & 0 & 0 & 0 & 0 & 0 & 0 & 0 & 0 & 0 \\
0 & 0 & 0 & 0 & 0 & 0 & 0 & \phi_y\widehat{\Gamma_3\bar{K}_{u3}}\phi_u^\dagger & \phi_y\widehat{\Gamma_3\bar{K}_{y3}}\phi_y^\dagger & 0 & 0 \\ \hline
0 & \phi\widehat{\Gamma_{p1}\bar{K}_{up1}}\phi^\dagger & 0 & 0 & \phi\widehat{\Gamma_{p2}\bar{K}_{up2}}\phi^\dagger & 0 & 0 & \phi\widehat{\Gamma_{p3}\bar{K}_{up3}}\phi^\dagger & 0 & I & \phi\widehat{\Gamma_p\bar{K}_{py}}\phi^\dagger \\
0 & \phi\widehat{\Gamma_{p1}\bar{K}_{up1}}\phi^\dagger & 0 & 0 & \phi\widehat{\Gamma_{p2}\bar{K}_{up2}}\phi^\dagger & 0 & 0 & \phi\widehat{\Gamma_{p3}\bar{K}_{up3}}\phi^\dagger & 0 & 0 & \phi\widehat{\Gamma_p\bar{K}_{py}}\phi^\dagger
\end{array}\right]}_{\mathbf{A_p}}
$$

$$
\underbrace{\left[\begin{array}{c} Y1_{r,j-1} \\ \delta U1_{r,j-1} \\ \delta Y1_{r,j-1} \\ \hline Y2_{r,j-1} \\ \delta U2_{r,j-1} \\ \delta Y2_{r,j-1} \\ \hline Y3_{r,j-1} \\ \delta U3_{r,j-1} \\ \delta Y3_{r,j-1} \\ \hline P_{r,j-1} \\ \delta P_{r,j-1} \end{array}\right]}_{\mathbf{xp_j}} + \underbrace{\left[\begin{array}{ccc}
\phi_y\widehat{H_1\phi_u^\dagger} & 0 & 0 \\
I & 0 & 0 \\
\phi_y\widehat{H_1\phi_u^\dagger} & 0 & 0 \\ \hline
0 & \phi_y\widehat{H_2\phi_u^\dagger} & 0 \\
0 & I & \\
0 & \phi_y\widehat{H_2\phi_u^\dagger} & 0 \\ \hline
0 & 0 & \phi_y\widehat{H_3\phi_u^\dagger} \\
0 & 0 & I \\
0 & 0 & \phi_y\widehat{H_3\phi_u}\dagger \\ \hline
\phi\widehat{H_{p1}}\phi^\dagger & \phi\widehat{H_{p2}}\phi^\dagger & \phi\widehat{H_{p3}}\phi^\dagger \\
\phi\widehat{H_{p1}}\phi^\dagger & \phi\widehat{H_{p2}}\phi^\dagger & \phi\widehat{H_{p3}}\phi^\dagger
\end{array}\right]}_{\mathbf{B_p}} \underbrace{\begin{bmatrix} \delta U1_{r,j} \\ \delta U2_{r,j} \\ \delta U3_{r,j} \end{bmatrix}}_{\mathbf{up_j}}
\tag{3-35}
$$

$$
\underbrace{\left[\begin{array}{c} Y1_{r,j} \\ Y2_{r,j} \\ Y3_{r,j} \\ \hline P_{r,j} \end{array}\right]}_{\mathbf{yp_j}} = \underbrace{\left[\begin{array}{ccccccccccc}
I & \phi_y\widehat{\Gamma_1\bar{K}_{u1}}\phi_u^\dagger & \phi_y\widehat{\Gamma_1\bar{K}_{y1}}\phi_y^\dagger & 0 & 0 & 0 & 0 & 0 & 0 & 0 & 0 \\
0 & 0 & 0 & I & \phi_y\widehat{\Gamma_2\bar{K}_{u2}}\phi_u^\dagger & \phi_y\widehat{\Gamma_2\bar{K}_{y2}}\phi_y^\dagger & 0 & 0 & 0 & 0 & 0 \\
0 & 0 & 0 & 0 & 0 & 0 & I & \phi_y\widehat{\Gamma_3\bar{K}_{u3}}\phi_u^\dagger & \phi_y\widehat{\Gamma_3\bar{K}_{y3}}\phi_y^\dagger & 0 & 0 \\ \hline
0 & \phi\widehat{\Gamma_{p1}\bar{K}_{up1}}\phi^\dagger & 0 & 0 & \phi\widehat{\Gamma_{p2}\bar{K}_{up2}}\phi^\dagger & 0 & 0 & \phi\widehat{\Gamma_{p3}\bar{K}_{up3}}\phi^\dagger & 0 & I & \phi\widehat{\Gamma_p\bar{K}_{py}}\phi^\dagger
\end{array}\right]}_{\mathbf{C_p}}
$$

$$
\underbrace{\left[\begin{array}{c} Y1_{r,j-1} \\ \delta U1_{r,j-1} \\ \delta Y1_{r,j-1} \\ Y2_{r,j-1} \\ \delta U2_{r,j} \\ \delta Y2_{r,j} \\ Y3_{r,j-1} \\ \delta U3_{r,j-1} \\ \delta Y3_{r,j-1} \\ \hline P_{r,j-1} \\ \delta P_{r,j-1} \end{array}\right]}_{\mathbf{xp_j}} + \underbrace{\left[\begin{array}{ccc}
\phi_y\widehat{H_1\phi_u^\dagger} & 0 & 0 \\
0 & \phi_y\widehat{H_2\phi_u^\dagger} & 0 \\
0 & 0 & \phi_y\widehat{H_3\phi_u^\dagger} \\ \hline
\phi\widehat{H_{p1}}\phi^\dagger & \phi\widehat{H_{p2}}\phi^\dagger & \phi\widehat{H_{p3}}\phi^\dagger
\end{array}\right]}_{\mathbf{D_p}} \underbrace{\begin{bmatrix} \delta U1_{r,j} \\ \delta U2_{r,j} \\ \delta U3_{r,j} \end{bmatrix}}_{\mathbf{up_j}}
\tag{3-36}
$$

where $\widehat{\phi\Gamma_{pi}\bar{K}_{pi}\phi^{\dagger}}$, $\widehat{\phi H_{pi}\phi^{\dagger}}$ with i=1,2 and 3 are obtained by properly partitioning the equation 3-34 for all the three blades. The above equations convert the control problem nicely into the standard discrete form. The next section 3-8 addresses the problem of tracking and derives the optimal control law required to meet the objective of driving the blade loads of the turbines to zero without affecting the total power production in a cycle.

3-8 LQ Tracker

It can be seen in the Equations 3-29, 3-30, 3-35, and 3-36 that we need to design the controller in such a way that the desired reference trajectory r(t) is tracked over a specified time interval (t_o, T). This section deals with deriving the optimal control law to meet the objectives. The given system to be tracked is in form:

$$x_{j+1} = Ax_j + Bu_j \tag{3-37}$$

$$y_j = Cx_j + Du_j \tag{3-38}$$

where y_j represents the output (which has to be tracked). Let the reference to be tracked is given by r_j. The error involved while tracking is given by:

$$e_j = y_j - r_j \tag{3-39}$$

The control strategy should be such that the error (e_j) goes to zero with time and a minimum control effort is used. A scalar performance can be given in a general form as shown (32):

$$J_j = \phi(N, x_N) + \sum_{j=1}^{N-1} L^j(x_j, u_j) \tag{3-40}$$

where [i,N] is the time interval with a fixed step size, $\phi(N, x_N)$ represents the cost incurred in the final time step and is a function of final state x_j and final time *N*, and $L^j(x_j, u_j)$ represents the cost at each intermediate time *k* in [i,N]. The control problem is to find an optimal u_k^* such that the performance index (J_j) is optimized. For the system given by equations 3-37 and 3-38, the scalar cost function in equation 3-40 can be given as:

$$J_j = \frac{1}{2}(e_N^T P e_N) + \frac{1}{2}\sum_{j=1}^{N-1}(e_j^T Q e_j + u_j^T R u_j) \tag{3-41}$$

where P, Q and R are semi positive definite matrices and represent the weights on the final state, the current state and the current input of the system respectively. Using equation 3-38 and 3-39, the cost function can now be written as:

$$\begin{aligned} J_j =& \frac{1}{2}[(Cx_N + Du_N - r_N)^T P(Cx_N + Du_N - r_N)] \\ +& \frac{1}{2}\sum_{j=1}^{N-1}[(Cx_j + Du_j - r_j)^T Q(Cx_j + Du_j - r_j) + u_j^T Ru_j] \end{aligned} \tag{3-42}$$

Using equations 3-40 and 3-42, we have:

$$\phi_j = \frac{1}{2}[(Cx_N + Du_N - r_N)^T P(Cx_N + Du_N - r_N)] \tag{3-43}$$

Lewis *et al.* (32) derived the optimal control by minimizing the following cost function:

$$\bar{J}_j = \frac{1}{2}[(Cx_N - r_N)^T P(Cx_N - r_N)] + \frac{1}{2}\sum_{j=1}^{N-1}[(Cx_j - r_j)^T Q(Cx_j - r_j) + u_j^T Ru_j] \tag{3-44}$$

The objective is to use a similar strategy to derive the optimal input by minimizing the cost function represented in equation 3-42. An augmented Lagrangian multiplier approach has been implemented (32) to minimize the performance index. Following the same approach, a Hamiltonian function is defined as:

$$H^j(x_j, u_j, \lambda_j) = \lambda_{j+1}^T x_{j+1} + L^j(x_j, u_j) \tag{3-45}$$

where λ is defined as Lagrange multiplier. Necessary conditions for a minimum can be achieved when the increments in the Hamiltonian function are equal to zero. The increments in the Hamiltonian function can be given as:

$$dH = H_x^T dx + H_u^T du + H_\lambda^T d\lambda \tag{3-46}$$

where $\quad H_x = \frac{\partial H}{\partial x}, \quad H_u = \frac{\partial H}{\partial u}, \quad H_\lambda = \frac{\partial H}{\partial \lambda}$

To fulfill the conditions of a minimum, *d*H should be made equal to zero.

$$x_{j+1} = \frac{\partial H^j}{\partial \lambda_{j+1}}, \quad j = i, ..., N-1 \tag{3-47}$$

$$\lambda_j = \frac{\partial H^j}{\partial x_j} = A^T \lambda_{j+1} + \frac{\partial L_j}{\partial x_j}, \quad j = i, ..., N-1 \tag{3-48}$$

$$0 = \frac{\partial H^j}{\partial u_j} = B^T \lambda_{j+1} + \frac{\partial L_j}{\partial u_j}, \quad j = i, ..., N-1 \tag{3-49}$$

where 3-47 is referred as *State equation*, 3-48 is termed as *Costate equation* and 3-49 is called as *Stationarity condition*. The importance of the Lagrange- multiplier can be analyzed here. In reality, the increments of *dx* and *du* are not independent. However, with the introduction of an extra degree of freedom i.e. Lagrange multiplier λ, it is possible for the increments of *dx* and *du* to behave independently (shown in equations 3-47, 3-48 and 3-49). The Lagrange multiplier has its own dynamics and is often termed as costate of the system. Moreover, it is also evident from the above equations that the state x_k develops recursively forward in time whereas λ develops recursively backwards in time (32). This accounts a two point boundary value problem, as an initial state x_i and a final costate λ_N are required for the solution of the above recursive equations. The boundary conditions derived in (32) are given as:

$$\left(\frac{\partial \phi}{\partial x_N} - \lambda_N\right)^T dx_N = 0 \quad and \tag{3-50}$$

$$\left(\frac{\partial H^j}{\partial x_i}\right)^T dx_i = 0 \tag{3-51}$$

As the initial state is known and fixed i.e. $dx_i = 0$, equation 3-50 will hold for any value of the Hamiltonian function (H_j). For the free-final state ($x_N \neq 0$), equation 3-51 reduces to:

$$\lambda_N = \frac{\partial \phi}{\partial x_N} \tag{3-52}$$

From equations 3-40 and 3-42, we can write:

$$L_j = \frac{1}{2}[(Cx_j + Du_j - r_j)^T Q(Cx_j + Du_j - r_j) + u_j^T Ru_j] \tag{3-53}$$

Similarly, from equations 3-45 and 3-37, it is clear that

$$H^j(x_j, u_j) = \lambda_{j+1}^T(Ax_j + Bu_j) + \frac{1}{2}[(Cx_j + Du_j - r_j)^T Q(Cx_j + Du_j - r_j) + u_j^T Ru_j] \tag{3-54}$$

Using equations 3-48 and 3-54, we have:

$$\lambda_j = A^T\lambda_{j+1} + C^T QCx_j - C^T Qr_j + Nu_j, \tag{3-55}$$

$$where\ N = C^T QD \tag{3-56}$$

Now using the equations 3-49 and 3-54, we have:

$$B^T\lambda_{j+1} + D^TQCx_j + D^TQDu_j - D^TQr_j + Ru_j = 0 \tag{3-57}$$

Solving for u_j, we have:

$$u_j = -\bar{R}^{-1}(B^T\lambda_{j+1} + N^Tx_j - D^TQr_j) \tag{3-58}$$

$$where\ \bar{R} = (R + D^TQD) \tag{3-59}$$

It can seen that the optimal control is a combination of a linear state variable feedback term along with a feedforward term depending on the reference and an extra term due to the feedthrough term in 3-38. Further, from equations 3-43, 3-52 and 3-56, it can be seen:

$$\lambda_N = C^TQCx_N - C^TQr_N + Nu_N \tag{3-60}$$

It can be seen from equation 3-30 that the control input in our problem formulation is the difference of the present and the past pitch angle. At the end of the control algorithm, we want the actual control input in equation 3-30 to converge to a constant pitch trajectory in a rotation which means that the difference in the set point for the pitch angle should be zero for last control horizon, i.e. u_N = 0, which reduces the equation 3-60 to :

$$\lambda_N = C^TQCx_N - C^TQr_N \tag{3-61}$$

From the above equation 3-61, that we can assume for all k $\leq$ N:

$$\lambda_j = S_jx_j - v_j \tag{3-62}$$

where S_j and v_j are still unknown sequences. Now, S_j is a $n \times n$ matrix and v_j is a n vector. Further, equations 3-37, 3-58 and 3-62 can be used to get:

$$x_{j+1} = Ax_j - B\bar{R}^{-1}B^T(S_{j+1}x_{j+1} - v_{j+1}) - B\bar{R}^{-1}N^Tx_j + B\bar{R}^{-1}D^TQr_j \tag{3-63}$$

which can be solved further to get

$$x_{j+1} = (I + B\bar{R}^{-1}B^TS_{j+1})^{-1}\Big[(A - B\bar{R}^{-1}N^T)x_j + B\bar{R}^{-1}B^Tv_{j+1} + B\bar{R}^{-1}D^TQr_j\Big] \tag{3-64}$$

Using equations 3-55 and 3-62 in the costate equation gives

$$S_jx_j - v_j = A^T\lambda_{j+1} + C^TQCx_j - C^TQr_j + Nu_j \tag{3-65}$$

Substituting the value of the optimal control input from equation 3-58 gives:

$$\begin{aligned} S_jx_j - v_j =& (A - B\bar{R}^{-1}N^T)^T\lambda_{j+1} + C^TQCx_j - C^TQr_j \\ & - N\bar{R}^{-1}N^Tx_j + N\bar{R}^{-1}D^TQr_j \end{aligned} \tag{3-66}$$

Using the costate equation from equation 3-62 leads to:

$$\begin{aligned} S_j x_j - v_j =& (A - B\bar{R}^{-1}N^T)^T(S_{j+1}x_{j+1} - v_{k+1}) + C^TQCx_j \\ &- C^TQr_j - N\bar{R}^{-1}N^Tx_j + N\bar{R}^{-1}D^TQr_j \end{aligned} \tag{3-67}$$

Further, utilizing the state equation from equation 3-63 gives us:

$$\begin{aligned} S_j x_j - v_j =& (A - B\bar{R}^{-1}N^T)^T\Big[S_{j+1}(I + B\bar{R}^{-1}B^TS_{j+1})^{-1}\Big[(A - B\bar{R}^{-1}N^T)x_j \\ &+ B\bar{R}^{-1}(B^Tv_{j+1} + D^TQr_j)\Big] - v_{j+1}\Big] + C^TQCx_j - C^TQr_j \\ &- N\bar{R}^{-1}N^Tx_j + N\bar{R}^{-1}D^TQr_j \end{aligned} \tag{3-68}$$

$$\begin{aligned} &\Big[- S_j + (A - B\bar{R}^{-1}N^T)^TS_{j+1}(I + B\bar{R}^{-1}B^TS_{j+1})^{-1}(A - B\bar{R}^{-1}N^T) + C^TQC - N\bar{R}^{-1}N^T\Big]x_j \\ &+ \Big[v_j + (A - B\bar{R}^{-1}N^T)^T\Big[S_{j+1}(I + B\bar{R}^{-1}B^TS_{j+1})^{-1}\Big(B\bar{R}^{-1}(B^Tv_{j+1} + D^TQr_j)\Big) - v_{j+1}\Big] \\ &- C^TQr_j + N\bar{R}^{-1}D^TQr_j\Big] = 0 \end{aligned} \tag{3-69}$$

This equation must hold for all states x_j for a given initial condition. This means that the bracketed terms must vanish individually. Using the matrix inversion lemma gives:

$$S_j = A_1^T[S_{j+1} - S_{j+1}B(B^TS_{j+1}B + \bar{R})^{-1}B^TS_{j+1}]A_1 + C^TQC - N\bar{R}^{-1}N^T \tag{3-70}$$

and

$$\begin{aligned} v_j =& A_1^T[S_{j+1} - S_{j+1}B(B^TS_{j+1}B + \bar{R})^{-1}B^TS_{j+1}][-B\bar{R}^{-1}(B^Tv_{j+1} + D^TQr_j] \\ &+ A_1v_{j+1} + (C^TQ - N\bar{R}^{-1}D^TQ)r_j \end{aligned} \tag{3-71}$$

where

$$A_1 = (A - B\bar{R}^{-1}N^T), \quad \bar{R} = R + D^TQD, \; and \quad N = C^TQD \tag{3-72}$$

The boundary conditions for these recursive equations can be derived from 3-61 and 3-62:

$$S_N = C^TPC, \tag{3-73}$$

$$v_N = C^TPr_N \tag{3-74}$$

As now the auxiliary matrices S_j and v_j can be computed recursively backwards in time with their known value in final time, the optimal control can now be computed as (from equation 3-37, 3-58 and 3-62):

$$u_j = -\bar{R}^{-1}[B^T S_{j+1}(Ax_j + Bu_j) - B^T v_{j+1} + N^T x_k - D^T Q r_k] \tag{3-75}$$

Further solving for the optimal control gives

$$u_j = (\bar{R} + B^T S_{j+1} B)^{-1}[-(N^T + B^T S_{j+1} A)x_j + B^T v_{j+1} + D^T Q r_j] \tag{3-76}$$

A *feedback gain* from the optimal control equation can be seen as:

$$K_j = (\bar{R} + B^T S_{j+1} B)^{-1}(N^T + B^T S_{j+1} A) \tag{3-77}$$

and a *feedforward gain* as:

$$K_j^v = (\bar{R} + B^T S_{j+1} B)^{-1} B^T \tag{3-78}$$

An extra feedforward term is introduced due to the feedthrough term:

$$K_j^{vd} = (\bar{R} + B^T S_{j+1} B)^{-1} D^T Q \tag{3-79}$$

The LQ Tracker is summarized in Algorithm 2. The algorithm stated offers a solution to the tracking problem represented by the equations 3-29, 3-30, 3-35 and 3-36 for the two control approaches proposed to meet the objectives. The Q matrix for the second approach which represents the weighting on the current states of the system can be decomposed into two parts (one for the blade loads and other for the total power in a rotation)

$$Q = \begin{bmatrix} Q_l & 0 \\ 0 & Q_p \end{bmatrix} \tag{3-91}$$

Here Q_l represents the weighting on the blade loads to track them to zero whereas Q_p is the weighting on the total power. In below rated wind speeds, where the focus is to extract maximum power from the wind turbine, higher weighting on the total power can be assigned whereas in above rated wind speeds, where the objective is to reduce the blade loads (to prevent the loads to cross the ultimate loads and reduce fatigue loads), higher weighting on the blade loads can be assigned. In this way, the second control approach offers a generic solution and can be valid for other wind speeds as well.

It is evident that once the LQ Tracker is applied to the equations 3-29, 3-30, 3-35 and 3-36 for the two control approaches, the optimal control gives the difference in the pitch activity for a period in the projected domain. Thus, a repetitive control law which gives the optimal input control sequence for the next iteration in the full domain is

Algorithm 2 LQ Tracker

State equation

$$x_{j+1} = Ax_j + Bu_j, \qquad j > i \tag{3-80}$$

Performance index

$$y_j = Cx_j + Du_j \tag{3-81}$$

$$J_j = \frac{1}{2}(y_N - r_N)^T P(y_N - r_N) + \frac{1}{2}\sum_{j=i}^{N-1}[(y_j - r_j)^T Q(y_j - r_j) + u_j^T R u_j] \tag{3-82}$$

Assumptions

$$P \geq 0, \qquad Q \geq 0, \qquad R \geq 0, \qquad with\ all\ three\ symmetric \tag{3-83}$$

Optimal control

$$A_1 = (A - B\bar{R}^{-1}N^T), \quad \bar{R} = R + D^T QD,\ and \quad N = C^T QD \tag{3-84}$$

$$S_j = A_1^T[S_{j+1} - S_{j+1}B(B^T S_{j+1}B + \bar{R})^{-1}B^T S_{j+1}]A_1 + C^T QC - N\bar{R}^{-1}N^T \tag{3-85}$$

$$\begin{aligned} v_j =& A_1^T[S_{j+1} - S_{j+1}B(B^T S_{j+1}B + \bar{R})^{-1}B^T S_{j+1}][-B\bar{R}^{-1}(B^T v_{j+1} + D^T Qr_j] \\ &+ A_1 v_{j+1} + C^T Qr_j - N\bar{R}^{-1}D^T Qr_j \end{aligned} \tag{3-86}$$

$$S_N = C^T PC, \qquad v_N = C^T Pr_N \tag{3-87}$$

$$K_j = (\bar{R} + B^T S_{j+1}B)^{-1}(N^T + B^T S_{j+1}A) \tag{3-88}$$

$$K_j^v = (\bar{R} + B^T S_{j+1}B)^{-1}B^T, \qquad K_j^{vd} = (\bar{R} + B^T S_{j+1}B)^{-1}D^T Q \tag{3-89}$$

$$u_j = -K_j x_j + K_j^v v_{j+1} + K_j^{vd} r_j \tag{3-90}$$

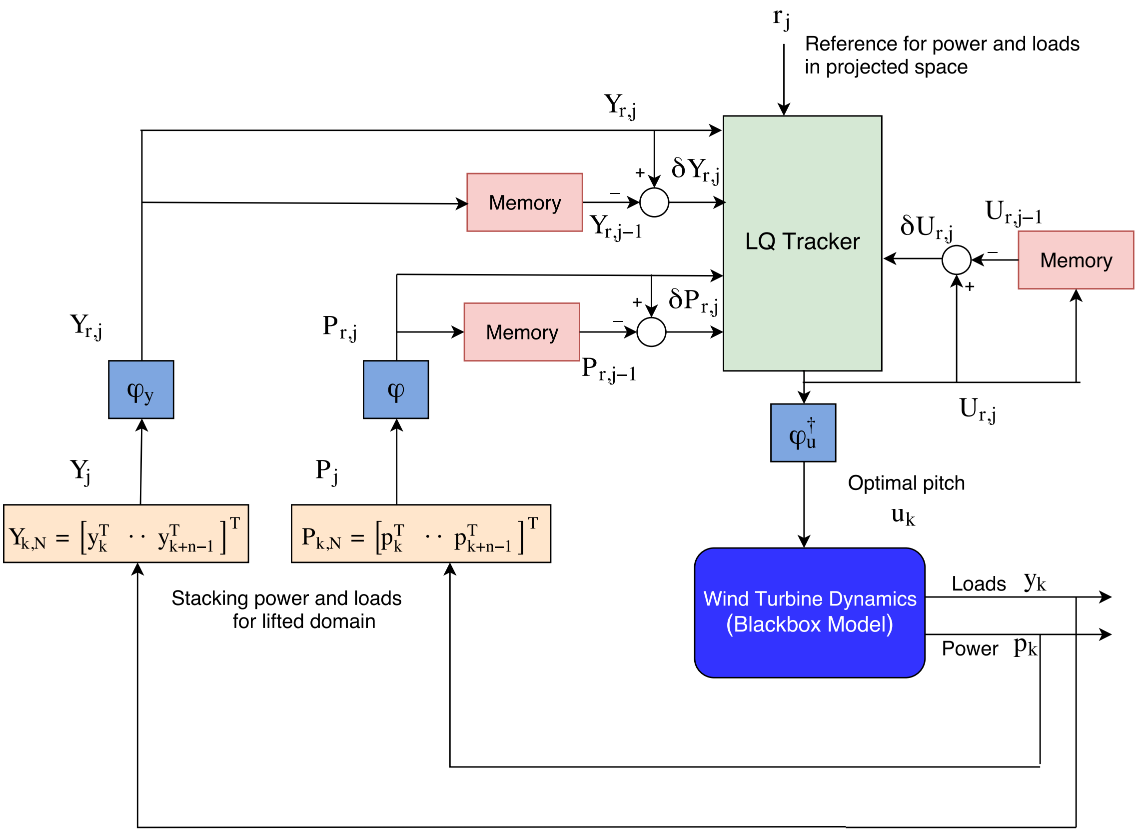

Figure 3-2: Implementation of SPRC technique

given in Equation 3-92. It should be noted that all variables in the equations presented in this chapter represent real numbers, unless noted otherwise. Figure 3-2 shows the complete implementation of SPRC technique with the LQ tracker.

$$U_{j,N} = U_{j-1,N} + \phi_u^\dagger \delta U_{r,j}^{*optimal} \tag{3-92}$$

Chapter 4

Results

This chapter presents the results of application of the theoretical framework to the wind turbine model. Before applying these concepts to the complicated non-linear wind turbine model, the concepts of lifted repetitive control and system identification in the reduced domain by the basis functions were tested on the simple test model named as Jeffcott Rotor. Further, these concepts were applied to the model of Vertical Axis Wind Turbine (VAWT). The two control approaches discussed in the previous chapter have also been implemented.

4-1 Jeffcott Rotor

A test case of Jeffcott rotor with the parameters, given in Table 4-1, was simulated. To simplify the analysis (as described in section 2-1), the motion of the rotor was decoupled in x and y directions. The disturbance input of 1P (1P means the fundamental frequency of rotor rotation) was added to a white noise to excite all the modes of rotor with the fundamental frequency. The system was allowed to run for 100 revolutions. Further, the basis functions with sines and cosines of 1P were taken. The input-output data was firstly converted into the lifted domain as explained in section 3-3 and then was translated into the projected space. Then the system identification using the Recursive Least Squares (RLS) was performed in the projected space (section 3-6).

As the basis functions for input and output were taken to be the same, size of the input and the output data in projected space was reduced to 2. While performing the identification process, the error for both the outputs in projected space (difference in the identified and simulated outputs) was calculated for every rotation and plotted as

Table 4-1: Parameters of Jeffcott Rotor

Mass of the disc (kg)	13.6
Eccentricity (m)	2×10^{-4}
Revolutions per minute (RPM)	6000
Stiffness (N/m)	2.92×10^{6}
Damping coefficient	1.36×10^{4}

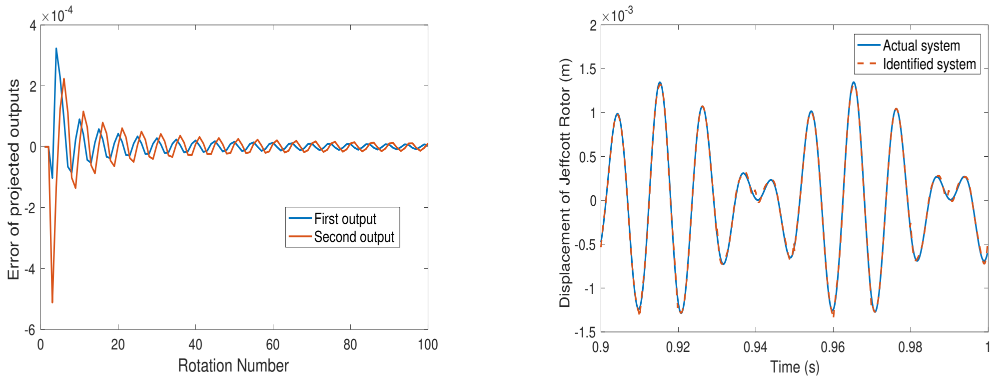

(a) SPRC identification in projected space

(b) Identification in last 10 revolutions

Figure 4-1: SPRC identification in Jeffcott rotor

shown in Figure 4-1a. The error in the outputs seemed to converge after around 60 rotations. After identifying the projected outputs, the identified outputs were translated back into the original space to check the fit of the input-output data. Figure 4-1b compares the identified and simulated outputs for last 10 revolutions and shows the convergence of Subspace Predictive Repetitive Control (SPRC) identification.

Once the SPRC identification worked successfully in the test case, these concepts were applied on the model of VAWT. The next sections describe the application of these concepts on the VAWT model.

4-2 Assumptions

It has to be noted that various assumptions were taken in the given model of VAWT which are listed as:

- The rotor speed is kept constant.
- Wind velocity are assumed constant (though some integrated white noise has been superimposed on the wind speed).

Table 4-2: VAWT specifications

Rated power (MW)	6
Number of blades	3
Radius of the blades (m)	90
Rated speed of rotor (RPM)	7.6
Rated wind speed (m/s)	12
Airfoil used	NACA0021
Position of rotor centre from ground (m)	90
Position of generator from ground (m)	30

- An ideal of pitch actuator is assumed (i.e. the actuator is assumed to track any specified pitch trajectory given by controller without any delay).
- As we are dealing with the Repetitive Controller, only rejection of periodic loads are considered.
- No structural flexibilities are considered.

The main reason behind these assumptions was to check and apply the concepts in Chapter 3 to a VAWT model with these assumptions. Further, the implementation of the control technique can be extended to a more realistic model of VAWT. The specifications of the VAWT model are summarised in Table 4-2.

4-3 Choice of basis functions

It is discussed in section 3-5 that sinusoidal basis functions are the suitable choice to capture the dynamics of the periodic systems. However, before determining the frequency content, it is necessary to know the time period of VAWT model. Figure 4-2a shows the variation of the blade loads in a rotation (with zero pitch input). The blade loads are 120 °symmetrically displaced with each other. It can be seen that for a given rotor speed, the time period of rotation is 10 seconds. Moreover, it can also be seen that the peak loading of blades occur in the upstream part. A sample time of 0.02 seconds was selected to capture the dynamics of VAWT. Figure 4-2b shows the Fourier analysis of the blade loads for 10 rotations. As the time period of rotation is 10 seconds, the fundamental period of frequency is 0.1 Hz. It can be seen that the energy of blade loads is distributed in 1P, 2P, 3P, 4P, 5P and 6P (where 1P represents the fundamental period i.e. 0.1 Hz). However, apart from these frequencies, contribution of zero frequency part to the blade loads can also be seen. The zero frequency part in Fourier domain refers to a constant. Thus, the basis functions of frequencies 1P, 2P, 3P, 4P, 5P, 6P and constant are required to capture the dynamics of the blade loads in the projected space. For the basis functions, we need the sines and cosines of these basis

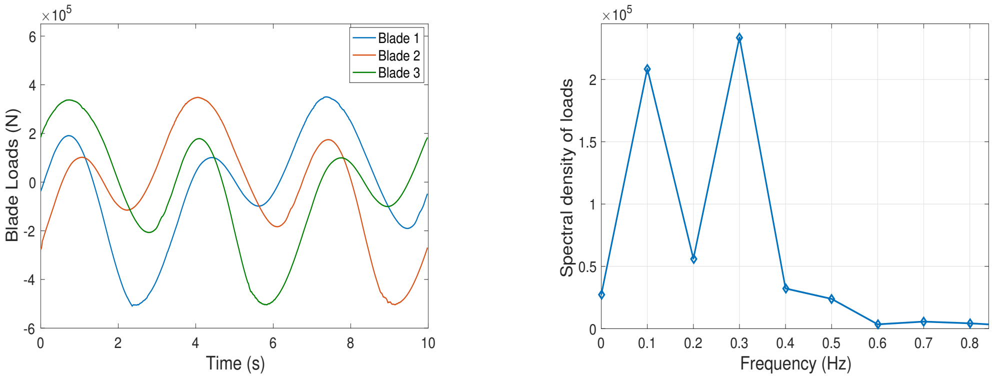

(a) Nature of blade loads **(b)** Fourier analysis of blade loads

Figure 4-2: Analysis of blade loads with no control

functions to cover all the phases of that particular frequency. Thus, 13 basis functions are used. As we have a sampling time of 0.02 seconds with 10 seconds of the rotational period, it gives 500 samples in a revolution. However, the use of basis functions reduce the large number of 500 to only 13 in projected space. The projected input-output data in every rotation actually represents the weights on the basis functions to recover the original shape.

4-4 System Identification

A proper excitation is needed for exciting all the modes of the reduced domain. As we have the frequency components from 1P-6P, an input signal which excites all the required frequencies is required. To fulfill this condition, a white noise signal was selected. Further, a bandpass filter is used which ensures the energy of the white noise is concentrated mostly in 1P-6P. The excitation signal for some rotations of turbine is shown in Figure 4-3a. Also, some process noise (i.e. some disturbance in the mean wind speed of 10 metres/second) has been added. An integrated white noise has been added to the constant wind speed to get a more realistic wind variation (Figure 4-3b). Further, system identification was performed using the recursive least squares approach along with a forgetting factor (as discussed in section 3-6). A low value of forgetting factor (like 0.95) increases the oscillations for the convergence of the norm of the identified parameters over rotations. So, a forgetting factor of 0.99 is used in the thesis. The identification algorithm was allowed to run for 60 rotor revolutions. The norm of the identified parameters was taken with every rotation and plotted (Figure 4-4a). It can be visualized that the norm of the identified parameters (for all the three blades) starts to converge after 50 rotations. However, it can be seen that even after 50 revolutions, the norm of the identified parameters oscillates a bit. This behaviour is due to the high

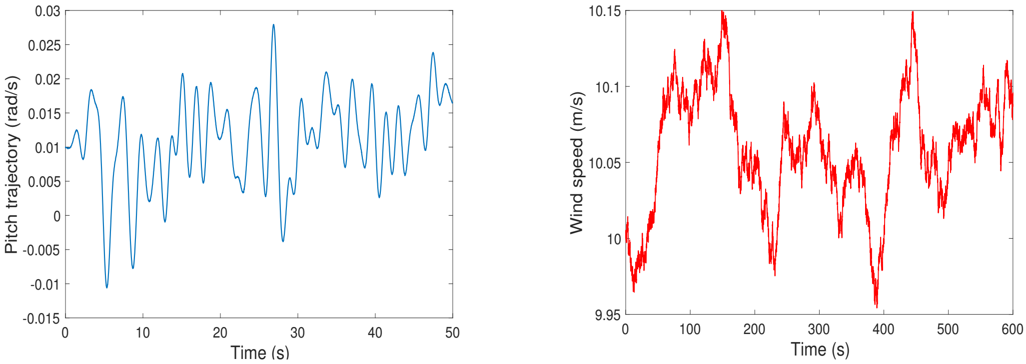

(a) White noise pitch signal for persistent excitation **(b)** Wind speed as an integrated white noise

Figure 4-3: Proper pitch excitation and integrated white noise on wind speed for wind turbine model

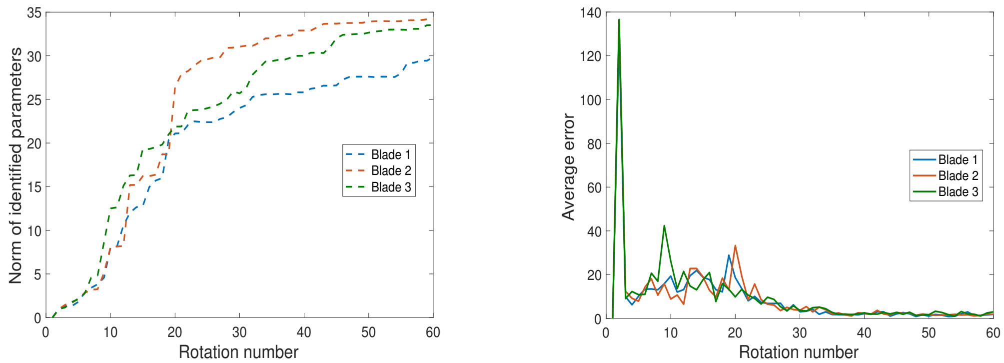

(a) Convergence of norm of identified parameters with the rotations **(b)** Convergence of averaged error in projected space over iterations

Figure 4-4: Convergence of SPRC identification with the rotations

frequency integrated white noise and the excitation signal which is also a bandpass white noise.

One of the other ways to look for the convergence of the identification algorithm is to focus on behaviour of the error in projected space with rotations (where error is the difference between the identified and simulated loads in projected space). There are 13 outputs in projected space (corresponding to 13 basis functions). So, the average of the absolute error in outputs in the projected space was taken in every rotation and plotted in Figure 4-4b. It is evident that the error started to converge to zero after 50 rotations. Moreover, the fit of the identified and the simulated outputs for 50th revolution in full space can be seen in Figure 4-5.

Further, to check the adaptive nature of the identification step, the mean wind speed

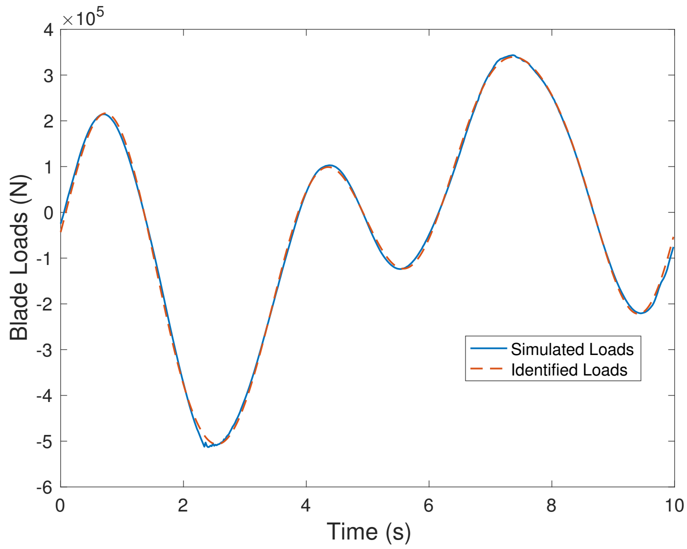

Figure 4-5: Comparison of identified and simulated blade loads for 50th rotation

was varied from 10 m/s to 11.5 m/s after 60 rotations. The effect on the identified parameters when the wind speed is varied can be seen in Figure 4-6. It can be visualized that when the wind is varied after 60 rotations, a peak in the averaged error of the projected loads is observed due to sudden change in wind dynamics. However, after 20 revolutions, the error starts to converge to zero. This aspect shows the adaptive nature of the SPRC identification.

It has been discussed that a bandpass white noise (with small constant for constant basis function) has been used for the excitation which makes the operating point of the linearized identified system as 0 radians. This means the best fit of the identified parameters would be achieved with no input applied. Now, the response of the identified parameters to the various pitch excitations is plotted and compared against the simulated responses.

It can be seen (from Figures 4-7, 4-8, 4-9) that as we increase the pitch angle (or go far away from the linearized operating point i.e. zero radians), the fit curve of the identified system deviates from the simulated loads of the simplified system. This result seems correct, as the identified parameters remain close to the true parameters only in the close vicinity of the operating point. But even, for high pitch angles like 0.08 radians (Figure 4-9a), the fitting of the curve is considered good enough for control purposes.

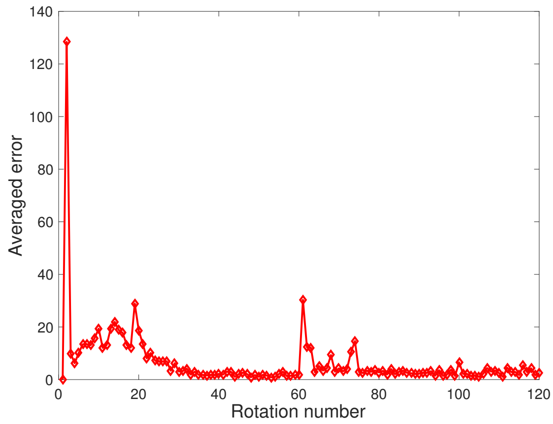

Figure 4-6: Convergence of identified parameters when wind speed is changed from 10 m/s to 11.5 m/s after 60 rotations

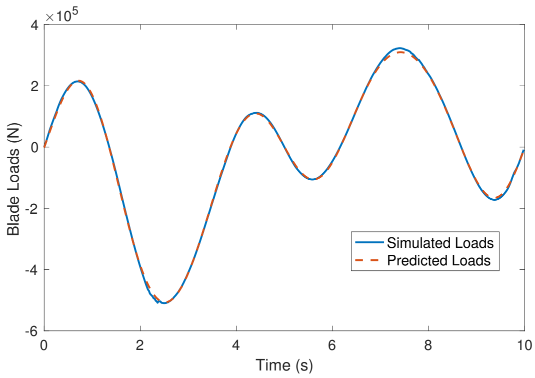

Figure 4-7: Comparing the predicted and simulated blade responses for zero pitch input

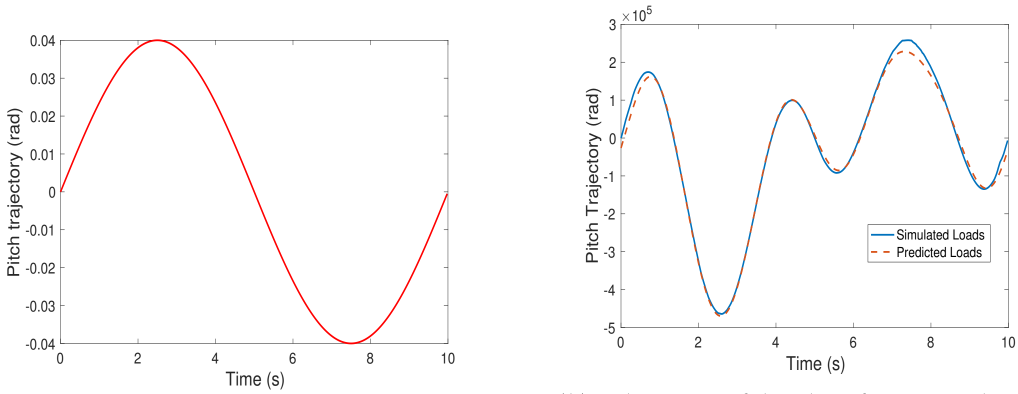

(a) Pitch trajectory to excite the blade loads

(b) Robustness of the identification with certain input

Figure 4-8: Comparing the predicted response with the actual response with the above pitch angle

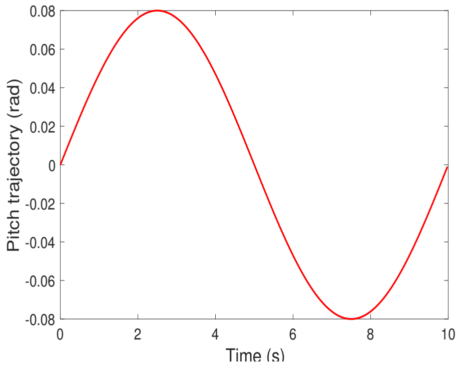

(a) Pitch trajectory to excite the blade loads

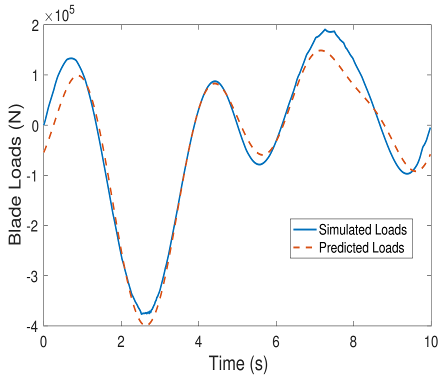

(b) Predicted blade responses for pitch input shown in Figure 4-9a

Figure 4-9: Comparing the predicted and simulated blade responses for pitch input shown in Figure 4-9a

4-5 Shaping the Blade Loads

It has been described that two control approaches have been implemented to achieve the control objective of reducing the normal peak load of the turbine without affecting the power production in the whole rotation. For the first approach, a reference was built to reduce the peak loads at the upstream side while increasing loads at the downstream side to ensure that the total power production per cycle is not affected. The reference was created using different weighting on the basis functions. One such reference which ensures the load transfer from upstream to downstream is shown in Figure 4-10. The aim of controller in projected space is to find the exact weights on the pitch trajectories (in projected space) using the basis functions to reach the optimal weighting of the blade loads to achieve the reference loads on the blades. Moreover, it is evident (from Figure 4-10) that the major difference in the reference and the identified system is particularly at two azimuth positions: one where we reduce the loads and second where we increase the loads. The use of basis functions with higher frequencies (3P, 4P, 5P and 6P) is possible, but increasing the frequencies will lead to higher cost of the actuator including the wear and loss of energy. Moreover, it will also result in high oscillations in the power curve. So, 1P, 2P and constant basis functions were used to achieve the objective. Figure 4-11 shows the optimal pitch trajectory when very low weights on 1P, 2P and constant basis function are used.

It can be seen in the controlled response (Figure 4-12) that the loads are decreased in the upstream but its compensation is in downstream. The results shows the reduction of the overall loads in upstream by 16.5%. Also, now the loads in upstream and downstream are more symmetrical. However, the power production per cycle is decreased by 4.89 %.

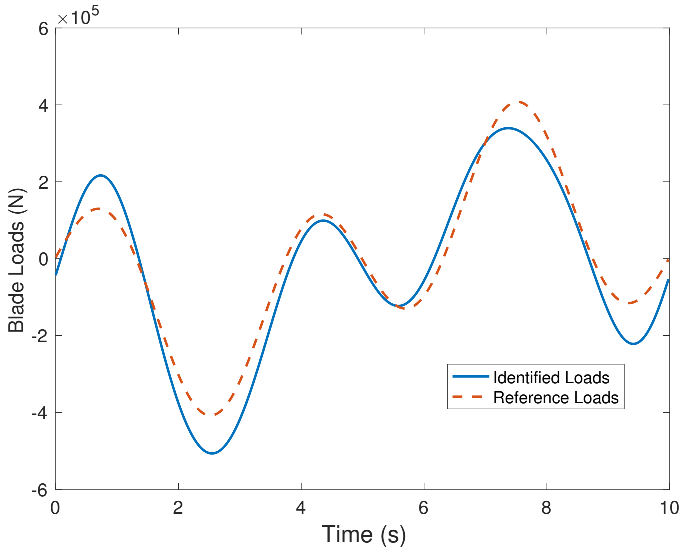

Figure 4-10: Load shaping of the reference loads

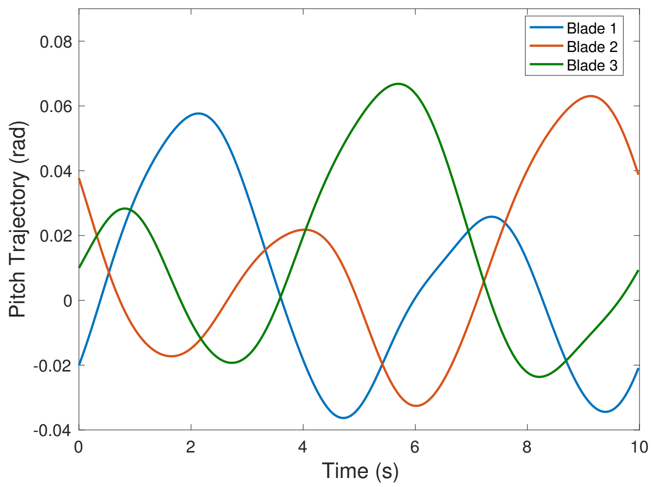

Figure 4-11: Control response for the blades with low weighting on constant, 1P and 2P basis functions

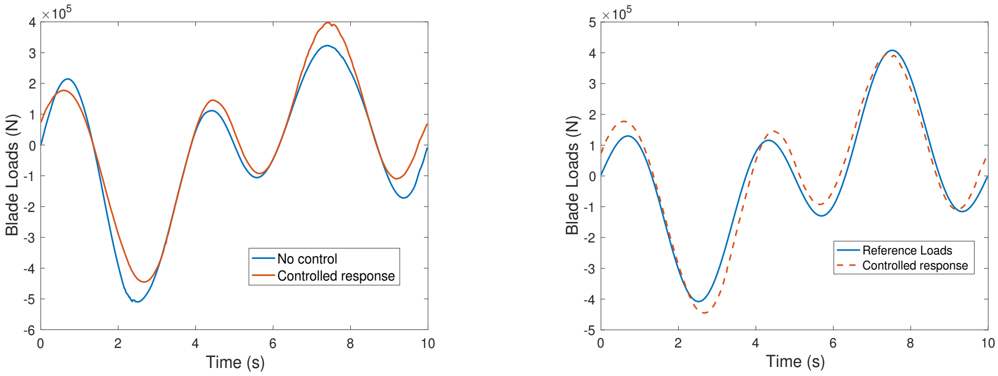

(a) Reduction of blade loads **(b)** Reference tracking using first control approach

Figure 4-12: Implementation of first control approach

4-6 Cost function including power and loads

Further, a second control approach which involves giving zero reference to the blade loads and giving total power per cycle as reference to the control was implemented. One of the reasons for adopting this generic type of strategy is that the controller has full freedom to choose the blade loads trajectory which meets the objective. Moreover, to avoid the contribution of high frequency basis functions, a significantly low weighting on the control input for 1P, 2P and 3P is used. Unlike the first control strategy, where three controllers were used to give the pitch angles for the three blades, this control approach uses a single control algorithm which gives the set point of the pitch angles for the blades. An optimized control pitch trajectory following this approach is obtained in Figure 4-13.

It can be seen that the pitch trajectories are symmetrically displaced by 120 $^\circ$ and have almost same amplitude. A control horizon of 5 iterations has been used to achieve the result. It has been shown in Section 4-4, that the predicted (from the identified model) and the simulated loads start to mismatch for high pitch angles. Due to this reason, the reference of 1.4 times the total power in a rotation was used as a reference. It is evident in Figure 4-14 that the value of cost function is decreasing continuously (and is minimum for 5th rotation) which shows the convergence of LQ Tracker. Further, the response of the simplified model, when this control input is applied can be seen as (Figure 4-15).

It is evident from Figure 4-16 that there is a reduction in blade loads of about 14.6% in 1P, 15.25 % in 2P and 5% reduction in 3P components of loads with no affect on the blade loads in zero frequency zone. However, to keep the power production same, the controller increases the loading in 5P frequency content of the loads. The response of power production to the controller can be seen in Figure 4-17 that the main decrease in power production corresponds to the decrease in peak loads in downstream side

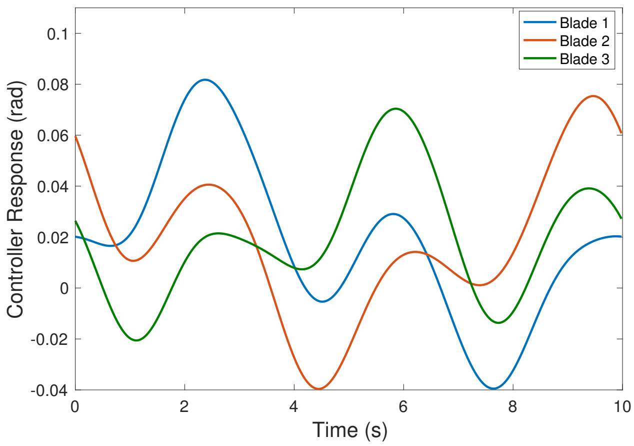

Figure 4-13: Pitch trajectory for the blades following second control strategy with high weighing on power production

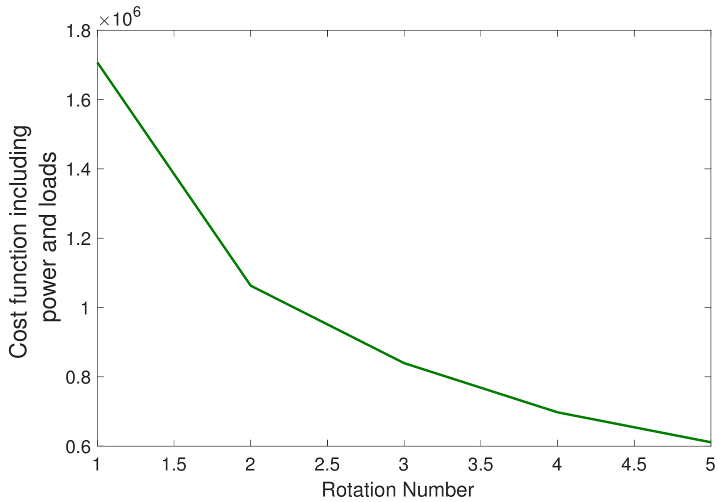

Figure 4-14: Cost function of LQ tracker using second control approach (high weight on power)

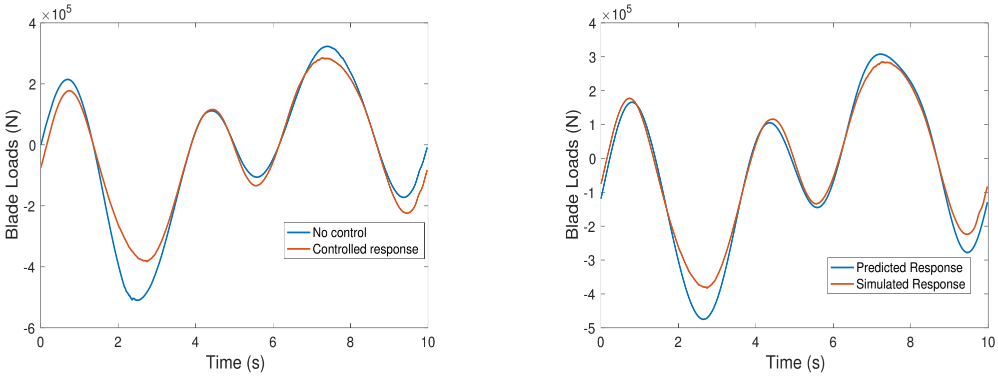

(a) Reduction of blade loads **(b)** Predicted and actual loads for second approach

Figure 4-15: Implementation of second control approach with high weighing on power production

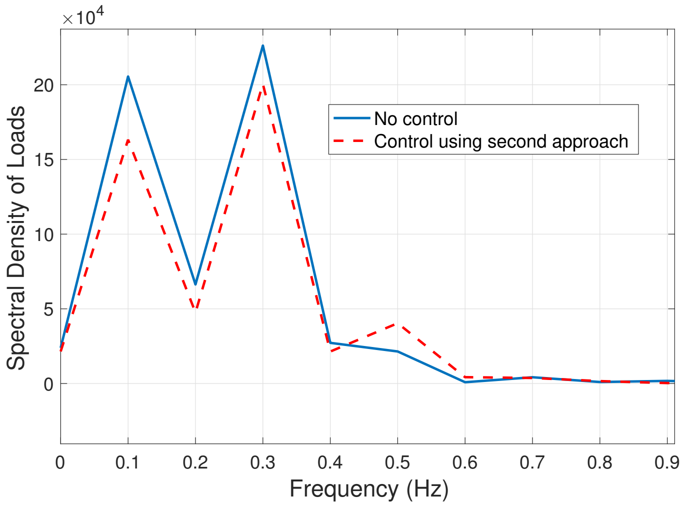

Figure 4-16: Analysis of frequency content in blade loads with and without control

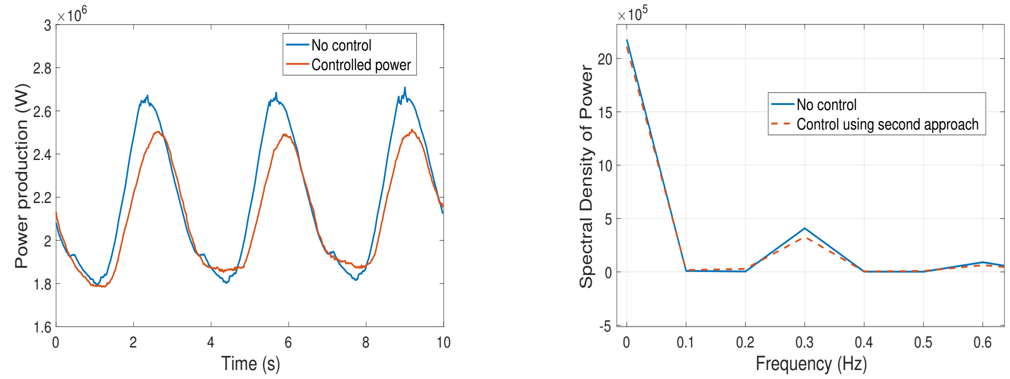

(a) Comparing the response of power with and without control

(b) Frequency spectrum of power with and without control

Figure 4-17: Effect of second control approach (with high weighting on power) on power production

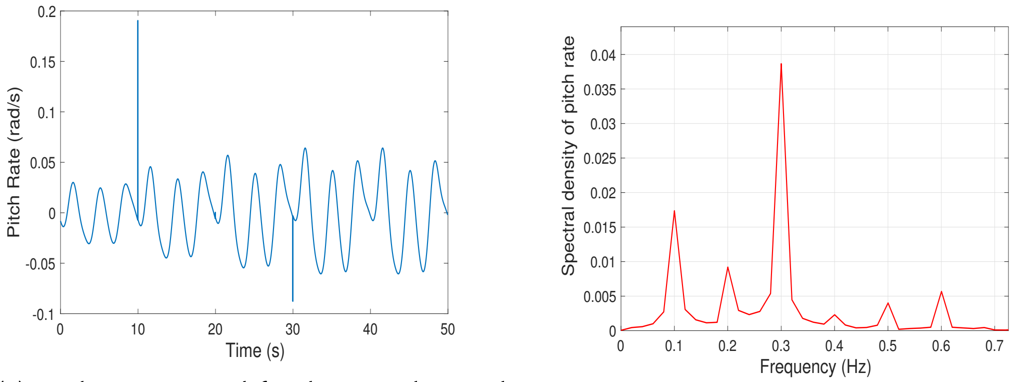

(a) Pitch rate required for the second control approach

(b) Frequency spectrum of pitch rate

Figure 4-18: Effect of second control approach (with high weighting on power) on pitch rate with control horizon of 5 rotations

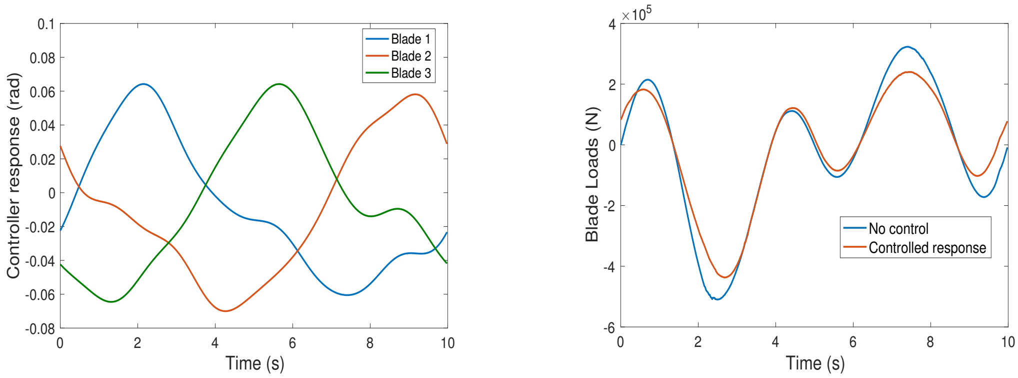

(a) Pitch trajectory for reducing the blade loads **(b)** Blade loads using high weighting on blade loads

Figure 4-19: Implementation of second control approach using high weighting on blade loads

of corresponding blades of turbine. It also shows that the main decrease in power is contributed by the 3P component. An ideal pitch actuator has been assumed for this thesis work. However, in reality, the pitch actuator has a maximum pitch rate it can produce to track the pitch set point by the controller. Generally, the maximum pitch rate for VAWT is around 10 ° per second. Figure 4-18a shows the pitch rate required and is well within the limits. However, at the end of rotations, a peak in the pitch rate is observed which can be smoothen over the rotations. It can also be seen (from Figure 4-18b) that a significant amount of 3P frequency is required to produce optimal pitching action on blades.

This control approach shows a significant amount of reduction of peak loads of 22 % with only 3.6 % of total power reduction per cycle. Moreover, the overall reduction of the blade loads is also considerably low as compared to the first control approach. Putting a higher weighting on the reference of blade loads in the second control strategy can significantly reduce the blade loads further but will also result in great power reduction. Figure 4-19a shows the optimal pitch trajectory to reduce the blade loads when a high weighting is imposed on the blade loads.

It is visible from Figure 4-19 that the blade loads reduced by 22 % in upstream and 35 % in the downstream part. However, there is a reduction of 18.7 % in the power in the whole rotation. This verifies that the control algorithm is working properly as it has lower weight on tracking of power production in a cycle. Hence, with a proper balance in the weighting of power and loads, the desired result can be obtained. All the results have been obtained for the mean wind speed of 10 m/s. It is also necessary to check if the identification and control is still applicable on wide range of wind speed as the behaviour of the wind turbine changes significantly even for small change in wind speed.

The mean wind speed is changed from 10 m/s to 11.5 m/s and after that to 7m/s to check the responses of the simplified model to the pitch trajectories obtained from

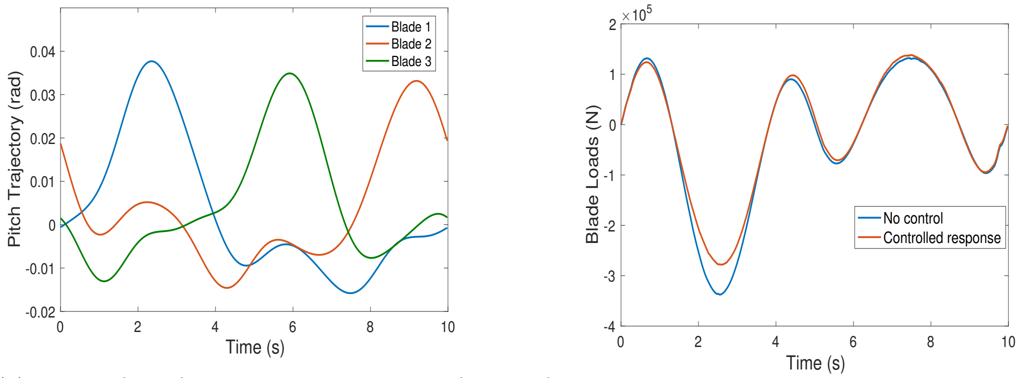

(a) Optimal pitch trajectory using second control approach **(b)** Reduction of blade loads with wind speed 7 m/s

Figure 4-20: Implementation of second control approach using high weighing on power production

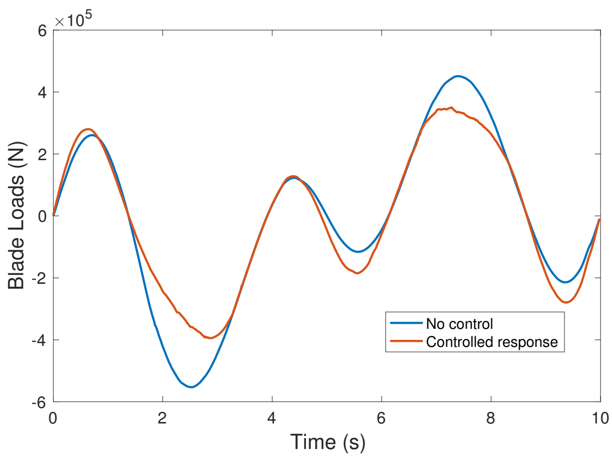

Figure 4-21: Response of the simplified model for wind speed of 11.5 m/sec with high weighing on power production

Table 4-3: Performance of VAWT

	Wind speed (7 m/s)	*Wind speed (10 m/s)*	*Wind speed (11.5 m/s)*
Peak reduction in upstream	26.5 %	22.4 %	21.5 %
Peak reduction in downstream	No affect	11.6 %	25.2 %
Reduction in power in a rotation	1.8 %	3.6 %	2.6 %

the controller. The peak load reduction of 20 % with 2.63 % of power reduction in the cycle was obtained with the wind speed of 11.5 m/s (Figure 4-21). When operating at wind speed of 7 m/s, peak load was reduced by 16.42 % with the power production per cycle reduction of only 1.78 % (Figure 4-12). This observation means that the system identification and controller are also working at the different wind speeds which gives more confidence in the controller synthesis. However, it should be noted that the re-identification of parameters was performed with changing wind speeds. The results for the performance of VAWT while using the second control approach (using high weight on power) can be summarized in Table 4-3.

4-7 First approach vs Second approach

The two control approaches have been implemented in the sections 4-5 and 4-6. Figure 4-22 compares the simulated response of simplified model of VAWT when pitch activities from both approaches are used as a control input. It can be seen from Table 4-4 that the first control approach reduces the peak loading of the upstream part but also increases the loading in downstream part with a total power loss of 5%. On the other hand, the second control approach (high weight on power) reduces the peak loading of the upstream as well as the downstream part with a significant part with only a small amount of power loss. Thus, the pitch trajectory offered by the second control approach is more optimal and gives significant potential of blade loads rejection without compromising the power.

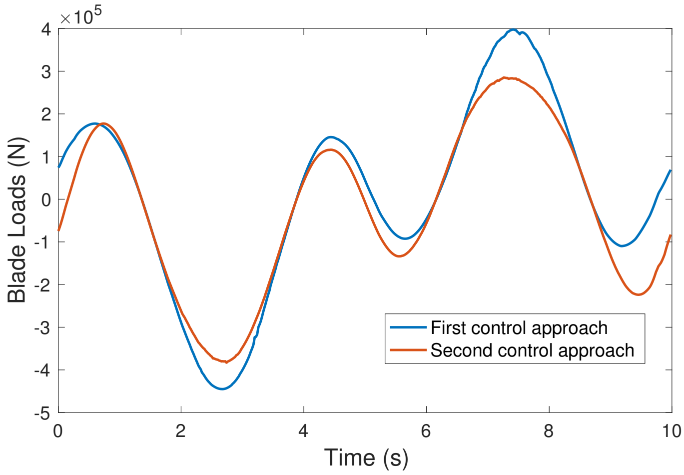

Figure 4-22: Performance of blade loads using both control approaches

Table 4-4: Comparing performance of VAWT using both control approaches

	First control approach	*Second control approach (high weighting on power)*
Peak reduction in upstream	16.5 %	22.4 %
Peak reduction in downstream	Increased by 17.3 %	11.6 %
Reduction in power in a rotation	4.9 %	3.6 %

Chapter 5

Conclusions & Future Work

5-1 Conclusions

The Subspace Predictive Repetitive Control (SPRC) has shown a lot of potential in achieving the control of Vertical Axis Wind Turbine (VAWT). As outlined earlier, two objectives were presented in the problem formulation which are answered in this section as:

- ***Performing data driven learning control on VAWT to ensure reduction of the periodic loading on the blades without compromising the power production per cycle.*** A proper pitch excitation with some noise excitation was sufficient enough to give a persistent excitation and further applying recursive least squares approach with forgetting factor aided in achieving the system identification. Further, based on the identified parameters, a successful control approach was developed (thus following the data-driven approach). However, as the identification of the parameters also involves some process noise, the estimated parameters are uncertain (depending on the level of noise). The proof of convergence of the identified parameters and thus the stability of the controlled system using data-driven approach still poses an open question for future research.

  The LQ tracker derived in section 3-8 has been successfully implemented in the control framework. It is evident in sections 4-5 and 4-6 that a significant load reduction has been achieved using the two control approaches. The second control approach is a generic solution to the research question as it gives the user the desired flexibility to decide the proper weighting to the load reduction and maintaining the same power in cycle. Unlike, in the first control approach, where the reference of the loads is already fixed, the controller does not have too much of the freedom to act. Using low weighting on the power production, it was also shown that not only the peak loads but also the loads at other azimuth positions were reduced, though a considerable loss in the power production per cycle was noticed. Thus, proper weighting can help us to achieve the different set of objectives.

- ***Reducing the complexity and the computational time of the control algorithm by performing the system identification and the controller synthesis in the reduced dimension.*** It has been shown in section 4-3 that the basis functions were able to reduce the number of samples in one rotation from 500 to only 13. Though the controller had only reduced space to act on, it was able to perform well. The system identification and the controller synthesis has been done in the reduced subspace thus achieving this objective.

5-2 Future Work

The work done in the thesis lays a foundation to further explore the possibilities of pitch controlled Vertical Axis Wind Turbines. There are several future recommendations for next steps based on the work done in the thesis as mentioned below:

- The speed of the rotor in the thesis has been assumed to be constant. However, in reality, it changes with the change in the wind speed. A next step can be to take into account the changing rotor speed. Changing basis functions according to the change in the rotor speed is the simplest solution for the changing rotor speed.
- Further, the next step can be to perform system identification and control simultaneously. As soon as the wind speed changes, the system identification would adaptively change its parameters and simultaneously the controller can take the actions accordingly, rather than waiting for the whole identification to finish.
- The work performed in this thesis assumed a constant wind direction. However, the change in the wind direction changes the angle of attack which can change the dynamics of the whole turbine.
- The thesis focused its attention on stand alone turbines. It would be useful to extend the analysis to the situation in a wind farm and study the effectiveness of the controller in optimizing the wind farm. The cost function can be changed by considering the total power production in the whole wind farm rather than taking the power from a single turbine. Similarly, the blade loads envelope of the

entire wind farm should be minimized, however it should be ensured that the peak loads do not cross the ultimate loads to ensure safe operation of the wind farm.

Bibliography

[1] O. Edenhofer, R. Pichs-Madruga, Y. Sokona, C. Field, V. Barros, T. F. Stocker, *et al.*, "Ipcc expert meeting on geoengineering meeting report," *Lima, Peru*, pp. 20–22, 2011.

[2] G. W. E. Council, "Global wind statistics 2016." , url: http://www.gwec.net/wp-content/uploads/vip/GWEC_PRstats2016_EN_WEB.pdf, last accessed on 18 August, 2017.

[3] Siemens, "Onshore wind power." , url: https://www.siemens.com/global/en/home/markets/wind/onshore.html, last accessed on 18 August, 2017.

[4] F. D. Bianchi, H. Battista, and R. J. Mantz, "Wind turbine control systems. advances in industrial control," 2007.

[5] W. Versteijlen, A. Metrikine, and K. van Dalen, "A method for identification of an effective winkler foundation for large-diameter offshore wind turbine support structures based on in-situ measured small-strain soil response and 3d modelling," *Engineering Structures*, vol. 124, pp. 221–236, 2016.

[6] J. S. Shamma, "An overview of lpv systems," in *Control of linear parameter varying systems with applications*, pp. 3–26, Springer, 2012.

[7] J. W. Van Wingerden, *Control of wind turbines with'Smart'rotors: Proof of concept & LPV subspace identification.* PhD thesis, TU Delft, 2008.

[8] S. T. Navalkar, J. W. van Wingerden, and T. Oomen, "Subspace predictive repetitive control with lifted domain identification for wind turbine individual pitch control," *IFAC Proceedings Volumes*, vol. 47, no. 3, pp. 6436–6441, 2014.

[9] L. Ljung, "On the estimation of transfer functions," *IFAC Proceedings Volumes*, vol. 20, no. 5, pp. 275–285, 1987.

[10] E. Mosca, *Optimal, predictive, and adaptive control*, vol. 151. Prentice Hall New Jersey, 1995.

[11] G. J. Van der Veen, *Identification of wind energy systems*. PhD thesis, TU Delft, 2013.

[12] G. Goodwin, P. Ramadge, and P. Caines, "Discrete-time multivariable adaptive control," *IEEE Transactions on Automatic Control*, vol. 25, no. 3, pp. 449–456, 1980.

[13] C. Kempf, W. Messner, M. Tomizuka, and R. Horowitz, "Comparison of four discrete-time repetitive control algorithms," *IEEE Control Systems*, vol. 13, no. 6, pp. 48–54, 1993.

[14] Y. Wang, F. Gao, and F. J. Doyle, "Survey on iterative learning control, repetitive control, and run-to-run control," *Journal of Process Control*, vol. 19, no. 10, pp. 1589–1600, 2009.

[15] G. A. Ramos, R. Costa-Castelló, and J. M. Olm, *Digital repetitive control under varying frequency conditions*, vol. 446. Springer, 2013.

[16] J.-X. Xu and R. Yan, "On repetitive learning control for periodic tracking tasks," *IEEE Transactions on Automatic Control*, vol. 51, no. 11, pp. 1842–1848, 2006.

[17] L. Mirkin and H. Rotstein, "On the characterization of sampled-data controllers in the lifted domain," *Systems & control letters*, vol. 29, no. 5, pp. 269–277, 1997.

[18] W. E. Larimore, "Canonical variate analysis in identification, filtering, and adaptive control," in *Decision and Control, 1990., Proceedings of the 29th IEEE Conference on*, pp. 596–604, IEEE, 1990.

[19] W. Favoreel, B. De Moor, and M. Gevers, "Spc: Subspace predictive control," *IFAC Proceedings Volumes*, vol. 32, no. 2, pp. 4004–4009, 1999.

[20] D. R. Tiwari, "Analysis of simple rotor system," *India: Institute of Technology Guwahati*, vol. 781039, 2008.

[21] Teachergeek, "Type of wind turbines." , url: http://teachergeek.org/wind_turbine_types.pdf, last accessed on 18 August, 2017.

[22] D. Vallverdu, *Study on vertical axis wind turbines using streamtube and dynamic stall models*. PhD thesis, Illinois Institute of Technology, 2014.

[23] I. Paraschivoiu, *Wind turbine design: with emphasis on Darrieus concept*. Presses inter Polytechnique, 2002.

[24] R. E. Gormont, "A mathematical model of unsteady aerodynamics and radial flow for application to helicopter rotors," tech. rep., Boeing Oeing Vertol Co Philadelphia PA, 1973.

[25] D. E. Berg, "Improved double-multiple streamtube model for the darrieus-type vertical-axis wind turbine," tech. rep., Sandia National Labs., Albuquerque, NM (USA), 1983.

[26] J. H. Strickland, B. Webster, and T. Nguyen, "A vortex model of the darrieus turbine: an analytical and experimental study," *Journal of Fluids Engineering*, vol. 101, no. 4, pp. 500–505, 1979.

[27] P. A. Kozak, D. Vallverdú, and D. Rempfer, "Modeling vertical-axis wind turbine performance: Blade element method vs. finite volume approach," in *To be submitted in the In Proceedings of The AIAA Propulsion and Energy Forum and Exposition*, vol. 2014, 2014.

[28] M. Ragheb, "Control of wind turbines," *URL: https://netfiles. uiuc. edu/mragheb/www/NPRE*, vol. 20475, 2008.

[29] B. Bamieh, J. B. Pearson, B. A. Francis, and A. Tannenbaum, "A lifting technique for linear periodic systems with applications to sampled-data control," *Systems & Control Letters*, vol. 17, no. 2, pp. 79–88, 1991.

[30] R. Kondor, "Regression by linear combination of basis functions," *New York:[sn]*, 2004.

[31] J. van de Wijdeven and O. H. Bosgra, "Using basis functions in iterative learning control: analysis and design theory," *International Journal of Control*, vol. 83, no. 4, pp. 661–675, 2010.

[32] F. L. Lewis, D. Vrabie, and V. L. Syrmos, *Optimal control.* John Wiley & Sons, 2012.

Glossary

List of Acronyms

HAWT	Horizontal Axis Wind Turbine
VAWT	Vertical Axis Wind Turbine
RLS	Recursive Least Squares
RC	Repetitive Control
GWEC	Global Wind Energy Council
COG	Center of Gravity
TSR	Tip Speed Ratio
ILC	Iterative Learning Control
LPV	Linear Parameter Varying
SPC	Subspace Predictive Control
SPRC	Subspace Predictive Repetitive Control
DMST	Double Multiple Streamtube Model
LTI	Linear Time Invariant
ECN	Energy research Centre of the Netherlands
DOF	Degree Of Freedom
BEM	Blade Element Momentum theory

List of Symbols

α	Angle of attack
β	Flight path angle
Γ	Extended observability matrix
ϕ_u	Input basis functions
ϕ_y	Basis functions for loads
τ	Unit vector tangential to blade
d_k	Periodic disturbance
d_w	Distance value in wake
e_k	Process noise
K_u	Extended controllability matrix
Q_l	Weighting on blade loads
Q_p	Weighting on total power in rotation
T_p	Rotational period
u_k	Input vector
u_r	Relative blade velocity
x_k	State vector
ϕ	Basis functions for power
D	Drag force
L	Lift force
N	Number of samples in a period
R	Radius of blade
R	Weighting on pitch angles